## METHODS

**Plasmids and reagents.** cDNA clones encoding mouse IGFBPs and *Xenopus* IGFBP-4 were purchased from Open Biosystems. XIGFBP-4-H74P mutant was generated with a QuickChange Site-Directed Mutagenesis kit (Stratagene). His-tagged human wild-type IGFBP-4 and mutant IGFBP-4-H74P (vectors provided by X. Qin)[8] were produced and purified with HisTrap HP Kit (Amersham). Full-length Frz8, Frz8CRD and LRP6N were provided by X. He[22,23]. Full-length LRP6, membrane-bound forms of LRP6 deletion mutants, and Dkk1 were from C. Niehrs[24]. pXwnt8 and pCSKA-Xwnt8 were from J. Christian[25]. pCS2–β-catenin was from D. Kimelman[26]. αMHC–GFP was from B. Fleischmann[27]. BRE–luc was from P. ten Dijke[28]. pCGN-Dvl-1 was described previously[29]. Soluble forms of LRP6 deletion mutants and probes for *in situ* hybridization analysis (Nkx2.5, cTnI and Hex) were generated by PCR. IGFBP-4, Wnt3A, IGF-I, IGF-II and BMP2 were from R&D. Neutralizing antibodies were from R&D (anti-IGFBP-4), Sigma (anti-IGF-I and anti-IGF-II), and Oncogene (anti-type-I IGF receptor). The antibodies used for immunoprecipitation, western blotting and immunostaining were from Invitrogen (anti-Myc, anti-V5), Santa Cruz (anti-cTnT, anti-IGFBP-4, anti-topoisomerase I (TOPO-I)), Sigma (anti-β-actin, anti-β-catenin, anti-FLAG (M2)) and Developmental Studies Hybridoma Bank (anti-sarcomeric myosin heavy chain (MF20)).

**Cell culture experiments.** P19CL6 cells and ES cells were cultured and induced to differentiate into cardiomyocytes essentially as described[6,10]. P19CL6 cells (2,000 cells per 35-mm dish) were treated with various conditioned media for screening of their cardiogenic activities. P19CL6 cells or ES cells stably transfected with αMHC promoter driven–GFP were generated by transfection of αMHC–GFP plasmid into P19CL6 cells or ht7 ES cells followed by G418 selection. Luciferase reporter gene assays, western blot analyses, immunostaining and RT–PCR were performed as described[10]. Reporter gene assays were repeated at least three times. PCR primers and PCR conditions are listed in Supplementary Table 1. For siRNA-mediated knockdown, siRNAs were expressed with pSIREN-RetroQ vector (Clontech). Oligonucleotide sequences used are listed in Supplementary Table 2. pSIREN-RetroQ vectors ligated with double-stranded oligonucleotides were transfected into P19CL6 cells or ES cells, and puromycin-resistant clones were isolated and expanded. For β-catenin stabilization assays, nuclear extracts of L cells were prepared with NE-PER Nuclear and Cytoplasmic Extraction Reagents (Pierce). Data are shown as means and s.d.

**IP/western blot analyses and binding assays.** Conditioned media for IP/western blot analyses containing full-length or various deletion mutants of IGFBPs, LRP6, Frz8CRD and Dkk1 were produced with 293 cells. Binding reactions were performed overnight at 4 °C. Immunoprecipitation was performed with Protein G–Sepharose 4 Fast Flow (Amersham). $^{125}$I-labelling of IGFBP-4 and Wnt3A was performed with IODO-BEADS Iodination Reagent (Pierce). A liquid-phase binding assay was performed essentially as described[19]. In brief, conditioned media containing LRP6N–Myc or Frz8CRD–Myc were mixed with various concentrations of $^{125}$I-labelled IGFBP-4 and incubated overnight at 4 °C. LRP6N–Myc or Frz8CRD–Myc was immunoprecipitated and the radioactivity of bound IGFBP-4 was measured after extensive washing of the Protein G–Sepharose beads. For a competitive binding assay, conditioned media containing LRP6N–Myc or Frz8CRD–Myc were mixed with $^{125}$I-labelled Wnt3A and unlabelled IGFBP-4, and incubated overnight at 4 °C. LRP6N–Myc or Frz8CRD–Myc was then immunoprecipitated and the radioactivity of bound Wnt3A was measured.

***Xenopus* experiments and mouse *in situ* hybridization analysis.** Axis duplication assays, animal cap assays and *in situ* hybridization analyses in *Xenopus* were performed essentially as described[20]. Two independent cDNAs for *XIGFBP-4*, presumably resulting from pseudotetraploid genomes, were identified by 5′ rapid amplification of cDNA ends (Supplementary Fig. 4a). Two different MOs targeting both of these two IGFBP-4 transcripts were designed (Gene Tools) (Supplementary Fig. 4a and Supplementary Table 2). MO-sensitive *XIGFBP-4* cDNA including a 41-base-pair 5′-untranslated region (UTR) was generated by PCR. MO-resistant *XIGFBP-4* cDNA (wild-type and H74P mutant) was generated by introducing five silent mutations in the MO1 target sequence and excluding the 5′-UTR (Supplementary Fig. 4a). To determine the specificity of MOs, MO-sensitive or MO-resistant *XIGFBP-4–myc* mRNA was injected into *Xenopus* embryos with or without MOs, and protein/mRNA expression was analysed. PCR primers and PCR conditions are listed in Supplementary Table 1. MOs and plasmid DNAs were injected at the eight-cell stage into the dorsal region of two dorsal–vegetal blastomeres fated to be heart and liver anlage. Electroporation of mRNA was performed essentially as described[21]. Injection of mRNA (5 ng in 5 nl of solution) into the vicinity of heart anlage and application of electric pulses were performed at stage 28. Whole-mount *in situ* hybridization analysis of murine IGFBP-4 was performed as described[30].


22. He, X. *et al.* A member of the Frizzled protein family mediating axis induction by Wnt-5A. *Science* **275**, 1652–1654 (1997).
23. Tamai, K. *et al.* LDL-receptor-related proteins in Wnt signal transduction. *Nature* **407**, 530–535 (2000).
24. Mao, B. *et al.* LDL-receptor-related protein 6 is a receptor for Dickkopf proteins. *Nature* **411**, 321–325 (2001).
25. Christian, J. L. & Moon, R. T. Interactions between Xwnt-8 and Spemann organizer signaling pathways generate dorsoventral pattern in the embryonic mesoderm of *Xenopus*. *Genes Dev.* **7**, 13–28 (1993).
26. Yost, C. *et al.* The axis-inducing activity, stability, and subcellular distribution of β-catenin is regulated in *Xenopus* embryos by glycogen synthase kinase 3. *Genes Dev.* **10**, 1443–1454 (1996).
27. Kolossov, E. *et al.* Identification and characterization of embryonic stem cell-derived pacemaker and atrial cardiomyocytes. *FASEB J.* **19**, 577–579 (2005).
28. Korchynskyi, O. & ten Dijke, P. Identification and functional characterization of distinct critically important bone morphogenetic protein-specific response elements in the Id1 promoter. *J. Biol. Chem.* **277**, 4883–4891 (2002).
29. Kishida, M. *et al.* Synergistic activation of the Wnt signaling pathway by Dvl and casein kinase Iε. *J. Biol. Chem.* **276**, 33147–33155 (2001).
30. Hosoda, T. *et al.* A novel myocyte-specific gene Midori promotes the differentiation of P19CL6 cells into cardiomyocytes. *J. Biol. Chem.* **276**, 35978–35989 (2001).

# Gremlin Enhances the Determined Path to Cardiomyogenesis

**Daisuke Kami[1,3], Ichiro Shiojima[4], Hatsune Makino[1], Kenji Matsumoto[2], Yoriko Takahashi[1], Ryuga Ishii[1], Atsuhiko T. Naito[4], Masashi Toyoda[1], Hirohisa Saito[2], Masatoshi Watanabe[3], Issei Komuro[4], Akihiro Umezawa[1]***

1 Department of Reproductive Biology, National Institute for Child Health and Development, Tokyo, Japan, 2 Department of Allergy and Immunology, National Institute for Child Health and Development, Tokyo, Japan, 3 Laboratory for Medical Engineering, Division of Materials Science and Chemical Engineering, Graduate School of Engineering, Yokohama National University, Yokohama, Japan, 4 Department of Cardiovascular Science and Medicine, Chiba University Graduate School of Medicine, Chiba, Japan

## Abstract

***Background:*** The critical event in heart formation is commitment of mesodermal cells to a cardiomyogenic fate, and cardiac fate determination is regulated by a series of cytokines. Bone morphogenetic proteins (BMPs) and fibroblast growth factors have been shown to be involved in this process, however additional factors needs to be identified for the fate determination, especially at the early stage of cardiomyogenic development.

***Methodology/Principal Findings:*** Global gene expression analysis using a series of human cells with a cardiomyogenic potential suggested *Gremlin* (*Grem1*) is a candidate gene responsible for *in vitro* cardiomyogenic differentiation. Grem1, a known BMP antagonist, enhanced DMSO-induced cardiomyogenesis of P19CL6 embryonal carcinoma cells (CL6 cells) 10–35 fold in an area of beating differentiated cardiomyocytes. The Grem1 action was most effective at the early differentiation stage when CL6 cells were destined to cardiomyogenesis, and was mediated through inhibition of BMP2. Furthermore, BMP2 inhibited Wnt/β-catenin signaling that promoted CL6 cardiomyogenesis.

***Conclusions/Significance:*** Grem1 enhances the determined path to cardiomyogenesis in a stage-specific manner, and inhibition of the BMP signaling pathway is involved in initial determination of Grem1-promoted cardiomyogenesis. Our results shed new light on renewal of the cardiovascular system using Grem1 in human.

**Citation:** Kami D, Shiojima I, Makino H, Matsumoto K, Takahashi Y, et al. (2008) Gremlin Enhances the Determined Path to Cardiomyogenesis. PLoS ONE 3(6): e2407. doi:10.1371/journal.pone.0002407

**Editor:** Hernan Lopez-Schier, Centre de Regulacio Genomica, Spain

**Received** January 15, 2008; **Accepted** May 5, 2008; **Published** June 11, 2008



**Funding:** This study was supported by a grant from the Ministry of Education, Culture, Sports, Science and Technology (MEXT) of Japan and Health and Labor Sciences Research Grants; by a Research grant on Health Science Focusing on Drug Innovation from the Japan Health Science Foundation; by the Program for Promotion of Fundamental Studies in Health Science of the Pharmaceuticals and Medical Devices Agency; by a grant from the Terumo Life Science Foundation; by a Research Grant for Cardiovascular Disease from the Ministry of Health, Labor and Welfare (MHLW); and by a Grant for Child Health and Development from the MHLW.

**Competing Interests:** The authors have declared that no competing interests exist.

* E-mail: umezawa@1985.jukuin.keio.ac.jp

## Introduction

The critical event in heart formation is commitment of mesodermal cells to a cardiomyogenic fate and their migration into anterolateral regions of the embryo during late gastrulation. In this process, morphogenic movements and cardiac fate determination are regulated by cytokines such as bone morphogenetic proteins (BMPs) [1–3], and fibroblast growth factors (FGFs) [4–7]. These secreted proteins from neighboring endoderm, ectoderm, and the mesoderm itself, play important roles in induction of cardiac transcription factors [8] and differentiation of cardiomyocytes in amphibians [9] and avians [4]. Cardiomyogenic signals, such as BMPs and FGFs, indeed activate expression of cardiac specific transcriptional factors (Csx/Nkx2.5, Gata4, Mef2c), and these transcriptional factors activate expression of circulating hormones (atrial natriuretic peptide (ANP), brain natriuretic peptide (BNP)), and cardiac specific proteins (myosin heavy chain (MyHC), myosin light chain (MyLC)). Wnt family proteins, cysteine-rich, and secreted glycoproteins, have also been implicated in embryonic development [10,11], and cardiomyogenesis [12,13]. In *Drosophila*, '*wingless*', a homologue of vertebrate Wnt is involved in expression of '*tinman*', a *Drosophila* homologue of Csx/Nkx2.5, through '*armadillo*', a *Drosophila* ortholog of β-catenin, and drives heart development [14]. In vertebrates, however, Wnt1/3a, which activates the canonical Wnt/β-catenin signaling pathway leading to stabilization of β-catenin as a downstream molecule through inactivation of glycogen synthase kinase-3β, inhibits cardiomyocytic differentiation from cardiac mesoderm [15–18]. Wnt11 promotes cardiac differentiation via the non-canonical pathway in *Xenopus* [12] and murine embryonic cell lines [19]. The secretion of Wnt inhibitors such as 'Cerberus', 'Dickkopf' and 'Crescent' by the anterior endoderm prevents Wnt3a secreted by the neural tube from inhibiting heart formation [15–17].

In this study, we performed GeneChip analysis to identify multiple extracellular determinants, such as cytokines, cell

membrane-bound molecules and matrix responsible for cardiomyogenic differentiation, and evaluated the statistical significance of differential gene expression by NIA array analysis (http://lgsun.grc.nia.nih.gov/ANOVA/) [20], a web-based tool for microarray data analysis. We found that Grem1 enhances the determined path to cardiomyogenesis in a stage-specific manner, and that inhibition of the BMP signaling pathway is, at least in part, involved in initial determination of Grem1-promoted cardiomyogenesis.

## Results

### GeneChip and statistical analysis

To identify cytokines and transcription factors responsible for cardiomyogenic differentiation, 69 human cells were analyzed, depending on gene expression levels, by GeneSpringGX software, and clustered into 30 groups (Fig. 1A, Table 1). Among the 30 groups, 21 groups included cells with a cardiomyogenic potential (Fig. 1B: red numbers). To identify genes specific for these groups, hierarchical clustering was employed, using the average distance method. Genes with the lowest average expression E(G1) within the cluster that can differentiate into cardiomyocytes and genes with the highest average expression E(G2) outside the cluster were identified, as previously described [20–22]. Genes which have E(G1)>E(G2) were estimated, using the False Discovery Rate (FDR<0.05). Grem1 was nominated as a cluster-specific cardiomyocyte-promoting gene in cells that could differentiate into cardiomyocytes following NIA array analysis (Fig. 1B). The gene expression profile reported in this paper has been deposited in the Gene Expression Omnibus (GEO) database (http://www.ncbi.nlm.nih.gov/geo: accession no. GSE8481, GSM41342-GSM41344, and GSM201137- GSM201145).

### Cardiomyogenic differentiation of CL6 cells with Grem1 and DMSO

To investigate cardiomyogenic activity of Grem1, P19CL6 embryonal carcinoma cells (CL6 cells) were used for assessment of *in vitro* cardiomyogenic differentiation, since CL6 cells are reproducibly and stably induced into beating cardiomyocytes by DMSO (Fig. 2Aa) [23]. CL6 cells did not differentiate following exposure to Grem1 alone at concentrations of 63 or 125 ng/ml for 14 days (Fig. 2B). However, Grem1 dramatically promotes DMSO-induced cardiomyogenic differentiation at a concentration of 63 and 125 ng/ml; Grem1 (125 ng/ml) especially increased DMSO-induced cardiomyogenic differentiation of CL6 cells as assessed by beating area (Fig. 2Ab and B) (Movie S1 and S2, http://1954.jukuin.keio.ac.jp/umezawa/kami/index.html).

### RT-PCR of differentiated or undifferentiated CL6 cells

To investigate gene expression as well as morphological analysis, i.e. beating, during cardiomyogenic differentiation, RT-PCR analysis was performed to detect expression of cardiomyocyte-specific/associate transcription factors, and structural genes (Fig. 2C). Genes encoding *Csx/Nkx2.5*, *Gata4*, *Hand2*, *Mef2c*, *ANP*, *BNP*, *MyLC-2a*, *MyLC-2v*, and *β-MyHC* were up-regulated during cardiomyogenic differentiation of CL6 cells treated with Grem1 and DMSO (Fig. 2C: lanes 6, 7 versus lane 3). Triplicate independent experiments confirmed the concentration-dependent Grem1 action on cardiomyogenic differentiation. The cardiomyocyte-specific genes (*Csx/Nkx2.5*, *Gata4*, *MyLC-2a*, *MyLC-2v*) expression level of CL6 cells treated with DMSO and Grem1 (63 and 125 ng/ml) were also the same as or higher than that of DMSO-induced CL6 cells by semi-quantitative RT-PCR (Figure S1).

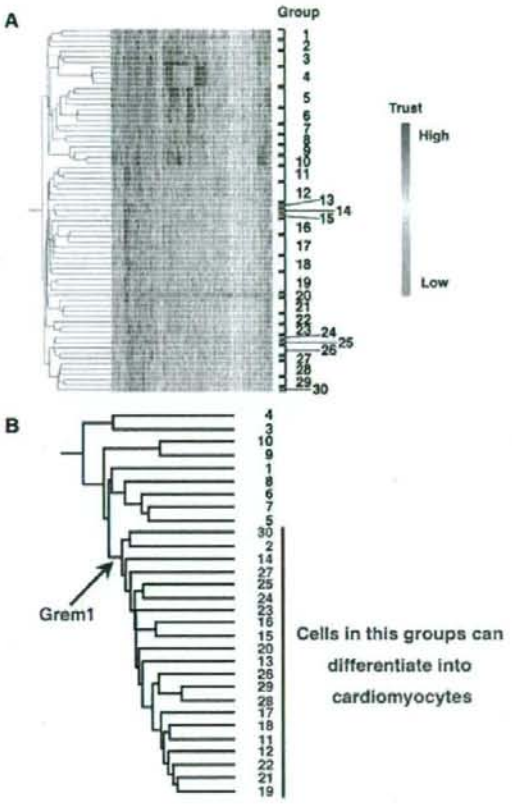


**Figure 1. Hierarchical clustering analysis on cultured human cells. (A)** Hierarchical clustering analyzed by GeneSpring. Based on gene expression pattern, 69 human cells were clustered into 30 sub-groups. The raw data from the GeneChip analysis are available at the GEO database with accession number GSE8481, GSM41342- GSM41344, and GSM201137- GSM201145. **(B)** Hierarchical clustering analysis was performed by NIA array (http://lgsun.grc.nia.nih.gov/ANOVA/), using averaged values of 30 sub-groups. Among the 30 groups, 21 groups included cells with a cardiomyogenic potential. To identify genes specific for these groups, hierarchical clustering was employed. *Grem1* was nominated as a cluster-specific cardiomyocyte-promoting gene in cells that could differentiate into cardiomyocytes.
doi:10.1371/journal.pone.0002407.g001

### Immunocytochemistry of differentiated or undifferentiated CL6 cells

To examine CL6 cells for expression of cardiomyocytic protein, immunocytochemical analysis was performed. CL6 treated with Grem1 (125 ng/ml) and DMSO exhibited clear striation with immunostain using anti-cTnT or anti-α-actinin (Fig. 2Da and b). The MF20- and cTnT-positive cells after exposure to Grem1 and DMSO formed clusters (Fig. 2Ea), compared with the cells after exposure to DMSO alone (Fig. 2Eb). CL6 cells treated with Grem1 alone were negative for MF20 and cTnT, but became positive for both markers following exposure to Grem1 (63 and 125 ng/ml) and DMSO (Fig. 2F). The beating area (Fig. 2B) showed a tendency similar to the MF20- and cTnT-positive area (Fig. 2F), thus there were positive correlations between them.

**Table 1.** 69 human cells clustered into 30 groups

| Group | | Title | Description | GSM |
|---|---|---|---|---|
| 1 | Normal epithelial cell,primary | NHEK-Neo1 | Normal epidermal keratinocyte, neonate, primary | GSM210361 |
| | | NHBE-1 | Normal bronchial epithelial cell, primary | GSM210362 |
| 2 | Pulmonary epithelial cell line | A549 | Pulmonary epithelial cell line | GSM210363 |
| | | BEAS-2B control (6hr) | Bronchial epithelial cell line | GSM210364 |
| 3 | Lymphocyte | RPMI8226control (6hr) | B cell line | GSM210365 |
| | | Raji-1 | B cell line | GSM210366 |
| | | NK92 | NK cell line | GSM210367 |
| 4 | Myelomonocytic leukemia | U937c | U937 control | GSM210368 |
| | | U937h | U937+HRF | GSM210369 |
| | | U937ha | U937+HRF+antibody | GSM210370 |
| | | U937a | U937+antibody | GSM210371 |
| 5 | Embryonal carcinoma, cancer | NCR-G3 | Embryonal carcinoma, NCR-G3, non-adherent | GSM201141 |
| | | NCR-G2NAd | Embryonal carcinoma, NCR-G2, non-adherent | GSM210373 |
| | | NCR-G4Ad | Embryonal carcinoma, NCR-G4, adherent | GSM201142 |
| | | NCR-G3Ad | Embryonal carcinoma, NCR-G3, adherent | GSM210375 |
| 6 | ES cell | H1_P43 | Undifferentiated hES | GSM41342 |
| | | H1-P46 | Undifferentiated hES | GSM41343 |
| | | H1-P41 | Undifferentiated hES | GSM41344 |
| 7 | Embryonal carcinoma, cancer | NCR-G2Ad | Embryonal carcinoma, NCR-G2, adherent | GSM201140 |
| | | NCR-G1 | Embryonal carcinoma, NCR-G3, non-adherent | GSM201139 |
| 8 | Ewing, cancer | NCR-EW2 | Ewing, cancer | GSM210378 |
| | | NCR-EW3 | Ewing, ETV4, cancer | GSM210379 |
| 9 | Ewing, cancer | GST6 | Ewing, POU5F1, cancer | GSM201137 |
| | | GST6-extra | Ewing, POU5F1, cancer | GSM210381 |
| 10 | Ewing, cancer | GST6-5az | Ewing, POU5F1, 5azaC, cancer | GSM201138 |
| | | GST6-5az-extra | Ewing, POU5F1, 5azaC, cancer | GSM210383 |
| 11 | Bone marrow cell, primary | H4-1 | Bone marrow cell, primary | GSM201143 |
| | | UBT5 | Bmi-1, hTERT, bone marrow cell | GSM210385 |
| | | UBET7 | Bmi-1, E6, hTERT, bone marrow cell | GSM210386 |
| 12 | Ligament-derived cells | #10 | Ligament, primary | GSM210387 |
| | Marrow stromal cells | H10-2Vec | Vector, bone marrow cell | GSM210388 |
| | | H10-2TERT | hTERT, bone marrow cell | GSM210389 |
| | | H10-2Bmi1 | Bmi-1, bone marrow cell | GSM210390 |
| 13 | Placenta, primary | PL90 | Placenta, primary | GSM210391 |
| 14 | De-differentiated chondrocyte | TdHC1 | E6, E7, hTERT, de-differentiated chondrocyte | GSM210392 |
| 15 | Neural differentiated marrow stromal cell | UET13 Neural differentiation | E7, hTERT, neural differentiation, bone marrow cell | GSM210393 |
| 16 | Neural differentiated marrow stromal cell | UET13 Neural differentiation1 | E7, hTERT, neural differentiation, bone marrow cell | GSM210394 |
| | | UET13 Neural differentiation4 | E7, hTERT, neural differentiation, bone marrow cell | GSM210395 |
| | | UET13 Neural differentiation5 | E7, hTERT, neural differentiation, bone marrow cell | GSM210396 |
| 17 | Cord blood-derived cells | UET13 | E7, hTERT, bone marrow cell | GSM210397 |
| | | UCB408 | Cord blood, primary | GSM210398 |
| | | UCB408E6E7-31 | E6, E7, umbilical cord blood | GSM210399 |
| | Adipocyte cell, primary | HAdPC1(5/21) | HAdpc1E6E7TERT28 | GSM210400 |
| 18 | Marrow mesenchymal cell, primary | UEET12 | E6, E7, hTERT, bone marrow cell | GSM210401 |
| | | UEE16 | E6, E7, bone marrow cell | GSM210402 |
| | | EPC hTERT+1 | E6, E7, hTERT, endometrial cell | GSM201144 |
| 19 | Cord blood, primary | UCB302 | Cord blood, primary | GSM210382 |
| | | UCB302-D7 | Cord blood, primary | GSM210405 |
| | | UCB302TERT | hTERT, cord blood | GSM210406 |
| | | UET9 | E7, hTERT, bone marrow cell | GSM210407 |

**Table 1.** cont.

| Group | | Title | Description | GSM |
|---|---|---|---|---|
| 20 | Cord blood, primary | UCB408E7-32 | E7, hTERT, cord blood | GSM210408 |
| 21 | Fetal fibroblast, primary | HFDPC cont. | Normal follicular dermal papillar cell, primary | GSM210409 |
| | | PL112 | Placenta, primary | GSM210410 |
| | | HF7-3 | Fetal fibroblast, primary | GSM210411 |
| 22 | Bone marrow cell, primary | 3F0664 | Bone marrow cell (commercial item), primary | GSM201145 |
| | | BM-MSC | Bone marrow-derived mesenchymal stem cells | GSM38627 |
| 23 | ES cell-derived mesenchymal cell | H1 clone 2 | ES cell-derived mesenchymal precursor | GSM38628 |
| | | H9 clone 1 | ES cell-derived mesenchymal precursor | GSM38629 |
| 24 | Endometrial cell | EPC100 | E6, E7, hTERT, endometrial cell | GSM210413 |
| 25 | Bone marrow cell, primary | Yub10F | Bone marrow cell, primary | GSM210414 |
| 26 | Endometrial cell | EPC hTERT+2 | E6, E7, hTERT, endometrial cell | GSM210415 |
| | | EPC Control | E6, E7, hTERT, endometrial cell | GSM210416 |
| 27 | Endometrial cell | EPC214 | E6, E7, hTERT, endometrial cell | GSM210417 |
| 28 | Menstruation blood-derived mesenchymal cell, primary | #E4 | Menstruation blood, primary | GSM210418 |
| | | #E4HRF | Menstruation blood, HRF treatment, primary | GSM210419 |
| | | #E5HRF | Menstruation blood, HRF treatment, primary | GSM210420 |
| 29 | Menstruation blood-derived mesenchymal cell, primary | #E6 | Menstruation blood, primary | GSM210421 |
| | | #E6HRF | Menstruation blood, HRF treatment, primary | GSM210422 |
| 30 | Menstruation blood-derived mesenchymal cell, primary | #E5 | Menstruation blood, primary | GSM210423 |

doi:10.1371/journal.pone.0002407.t001

## Grem1 and DMSO were most effective at the early stage (days 1–3) of CL6 differentiation

To determine if Grem1 (125 ng/ml) functions during the early or the late stage of differentiation, CL6 cells were treated with Grem1 for different time periods (Fig. 3A). Grem1 and DMSO were most effective on CL6 differentiation at 1–3 days (Fig. 3B, C) as assessed by percentages of MF20-positive area and beating area. Since Grem1 inhibits BMPs through direct binding [24], we hypothesized that BMP signaling is inhibitory to CL6 cardiomyogenesis during days 1–3. To confirm this hypothesis, RT-PCR analysis was performed to determine expression of the early mesodermal marker (*BrachyuryT* and *Tbx6*), cardiomyocyte-specific transcription factors (*Csx/Nkx2.5*), structural genes (*β-MyHC*), and *Gapdh* (Fig. 4A). DMSO induced the *BrachyuryT* and *Tbx6* genes, and their expressions peaked at 3 days and then decreased; BMP2 down-regulated expression of these genes at 3–7 days. The *Csx/Nkx2.5* and *β-MyHC* genes started to be expressed at days 3 and 5, respectively, and their expression increased up to 14 days, at which time the timeframe analysis was terminated. BMP2 clearly inhibited expression of the *Csx/Nkx2.5* and *β-MyHC* genes (Fig. 4A, lanes 1–7 versus lanes 8–14).

To examine cardiomyogenic differentiation, immunocytochemical analysis was performed on CL6 cells treated with the inducers. CL6 cells treated with DMSO and BMP2 for the first 3 days were negative for sarcomeric myosin (MF20) at 14 days, but became positive for sarcomeric myosin, following exposure to DMSO alone during days 1–3 (Fig. 4B). To determine if DMSO induces BMP production in CL6 cells, expression levels of *Bmp2* and *Bmp4* were determined by quantitative real-time RT-PCR analysis (Fig. 4C). DMSO clearly induced the *Bmp2* and *Bmp4* genes, and DMSO-induction was inhibited by BMP2 protein. The expression level of *Bmp2* was highest during days 7–10 (Fig. 4C: *Bmp2*) in DMSO-induced CL6 cells, and that of *Bmp4* was highest during days 5–7 (Fig. 4C: *Bmp4*).

To investigate BMP signaling on cardiomyogenic differentiation, we used the *Id1* promoter-Lux plasmid that includes the luciferase gene driven by the *Id1* promoter, known as a BMP target promoter (Fig. 4D). DMSO increased BMP signaling activity that peaked at 5 days (Fig. 4D, open square). BMP2 protein increased BMP signaling activity at 3 days (Fig. 4D, closed square), but lost BMP signaling activity at 5 days and later, implying that this loss of BMP signaling leads to lack of cardiomyogenic induction.

Since Wnt/β-catenin signaling is involved in CL6 cardiomyogenesis [23,25], we hypothesized that the BMP effect on CL6 cardiomyogenesis is mediated through Wnt/β-catenin signaling. Expression of Wnt3a, an activator of canonical Wnt signaling, was indeed detected in CL6 cells exposed to DMSO, and BMP2 significantly down-regulated *Wnt3a* expression at day 3 (Fig. 4E). By using the TOPflash plasmid [23] which includes the luciferase gene driven by two sets of three copies of the TCF recognition site, Wnt/β-catenin signaling was assessed to investigate the effect of BMP2. Wnt/β-catenin signaling activity increased at 48 h after treatment with DMSO. Activity was increased by DMSO treatment but decreased by BMP2 (Fig. 4F). Time course analysis revealed that Wnt/β-catenin activity peaked at 5 days after DMSO treatment, and decreased thereafter (Fig. 4G). BMP2 inhibited DMSO-induced Wnt/β-catenin activity throughout the experimental period (up to 14 days). These results imply that BMP signaling inhibits CL6 cardiomyogenesis at the early stage through inhibition of Wnt/β-catenin signaling.

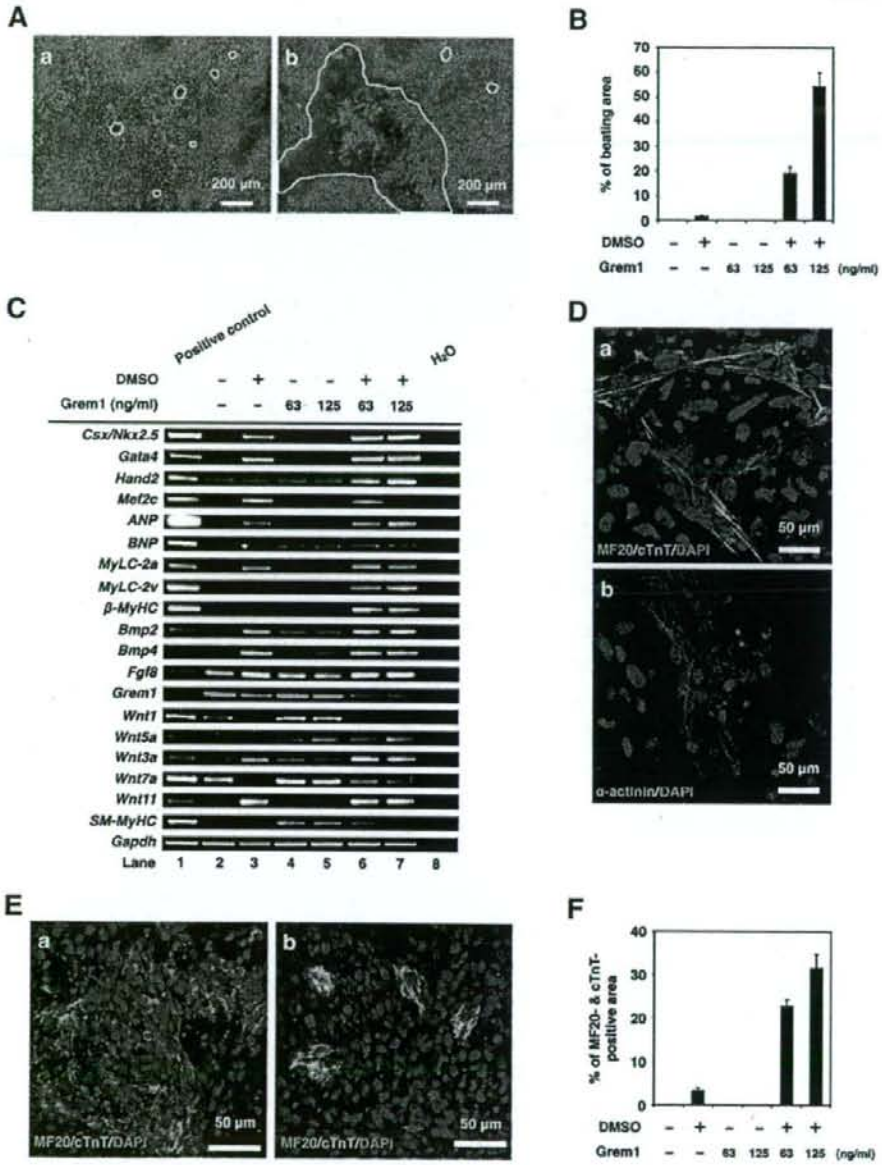


**Figure 2. Grem1 enhanced cardiomyogenic differentiation in DMSO-induced CL6 cells. (A)** Phase contrast micrograph of CL6 cells with exposure to DMSO alone (a), Grem1 (125 ng/ml) and DMSO (b) for 14 days. The medium, including Grem1 and DMSO, was changed every day. CL6 cells exhibited apparent spontaneous beating between days 9–11. Beating CL6 cell colonies are outlined by white lines. **(B)** Percentage of beating area in differentiated CL6 cells. CL6 cell treated with Grem1 (125 ng/ml) and DMSO exhibited the strongest contraction. **(C)** RT-PCR analysis of the genes encoding cardiac-specific transcriptional factors (*Csx/Nkx2.5, Gata4, Mef2c, Hand2*), circulating hormone (*ANP, BNP*), cardiac-specific proteins (*MyLC-2a, MyLC-2v, β-MyHC*), cytokines (*Bmp2, Bmp4, Fgf8, Grem1, Wnt1, Wnt3a, Wnt5a, Wnt7a, Wnt11*), *SM-MyHC*, and *Gapdh* (From top to bottom). Mouse total heart RNA for the *Csx/Nkx2.5, Gata4, Mef2c, Hand2, ANP, BNP, MyLC-2a, MyLC-2v, β-MyHC, Bmp2, Bmp4, Grem1, Wnt11, SM-MyHC*, and *Gapdh* genes, mouse embryonic stem cell RNA for the *Fgf8* gene, and mouse total skeletal muscle RNA for the *Wnt1, Wnt3a, Wnt5a*, and *Wnt7a* genes were used for positive controls. $H_2O$ (without RNA) served as a negative control. **(D)** Immunocytochemistry of CL6 cells 14 days after exposure to Grem1 (125 ng/ml) and DMSO with MF20 and cTnT (a), and α-actinin (b). Cell nuclei are stained with DAPI. Clear striations are evident. **(E)** Immunocytochemistry of CL6 cells 14 days after exposure to Grem1 and DMSO with cardiac troponin T (cTnT) and sarcomeric myosin (MF20). CL6 cells treated with Grem1 (125 ng/ml) and DMSO (a), and DMSO alone (b) stained positive for cTnT and MF20. Untreated CL6 cells, i.e. not exposed to Grem1(125 ng/ml) or DMSO, stained negative for cTnT and MF20. Cell nuclei were stained with DAPI. **(F)** Percentage of MF20- and cTnT-double positive area.
doi:10.1371/journal.pone.0002407.g002

**A**

| | Day | 0 | 1 | 2 | 3 | 4 | 5 | 6 | 7 | 8 | 9 | 10 | 11 | 12 | 13 | 14 |
|---|---|---|---|---|---|---|---|---|---|---|---|---|---|---|---|---|
| DMSO | – | – | – | – | – | – | – | – | – | – | – | – | – | – | – | – |
| Grem1 | – | – | – | – | – | – | – | – | – | – | – | – | – | – | – | – |
| DMSO | 1-14 | – | + | + | + | + | + | + | + | + | + | + | + | + | + | + |
| Grem1 | – | – | – | – | – | – | – | – | – | – | – | – | – | – | – | – |
| DMSO | 1-14 | – | + | + | + | + | + | + | + | + | + | + | + | + | + | + |
| Grem1 | 1-3 | – | + | + | + | – | – | – | – | – | – | – | – | – | – | – |
| DMSO | 1-14 | – | + | + | + | + | + | + | + | + | + | + | + | + | + | + |
| Grem1 | 4-7 | – | – | – | – | + | + | + | + | – | – | – | – | – | – | – |
| DMSO | 1-14 | – | + | + | + | + | + | + | + | + | + | + | + | + | + | + |
| Grem1 | 8-14 | – | – | – | – | – | – | – | – | + | + | + | + | + | + | + |
| DMSO | 1-3 | | + | + | + | – | – | – | – | – | – | – | – | – | – | – |
| Grem1 | – | – | – | – | – | – | – | – | – | – | – | – | – | – | – | – |
| DMSO | 1-14 | – | + | + | + | + | + | + | + | + | + | + | + | + | + | + |
| Grem1 | 1-14 | – | + | + | + | + | + | + | + | + | + | + | + | + | + | + |
| DMSO | 1-14 | – | + | + | + | + | + | + | + | + | + | + | + | + | + | + |
| Grem1 | 1-3 | – | + | + | + | – | – | – | – | – | – | – | – | – | – | – |
| DMSO | 1-3 | – | + | + | + | – | – | – | – | – | – | – | – | – | – | – |
| Grem1 | 1-3 | – | + | + | + | – | – | – | – | – | – | – | – | – | – | – |

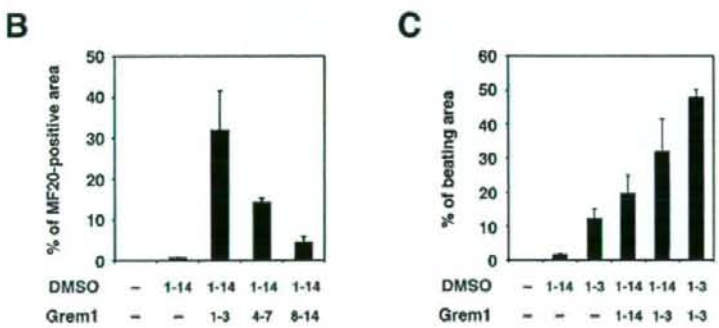


**Figure 3. Percentage of myogenic differentiation by period of treatment with Grem1 in CL6 cells. (A)** Protocol for treatment of Grem1 and DMSO. CL6 cells were passaged at $1.8\times10^5$ cells in 6-well plate on Day 0. CL6 cells were exposed to Grem1 (125 ng/ml) and/or DMSO on the indicated day. Day when the cells were exposed to the inducers is shown by "+" (in gray cells for clarity). The medium including Grem1 and DMSO was changed every day. On day 14, the cells were immunocytochemically stained with MF20 antibody. **(B)** Myogenic differentiation of CL6 cells was estimated by sarcomeric myosin (MF20)-positive area. CL6 cells were treated with Grem1 (125 ng/ml) and DMSO for the indicated days. **(C)** Myogenic differentiation of CL6 cells was estimated by beating area. CL6 cells treated with DMSO and Grem1 (125 ng/ml) were incubated at indicated days.
doi:10.1371/journal.pone.0002407.g003

## Discussion

Our bioinformatics study using the results from the global gene expression analysis of human cells (GSM412342-41344 and GSM201137-201145 at http://www.ncbi.nlm.nih.gov/geo) nominated Grem1 as a candidate gene that may participate in cardiomyogenesis. By using CL6 embryonic cells as a model of cardiomyogenesis, we obtained two major findings: the first is that Grem1 enhanced cardiomyogenic differentiation of DMSO-induced CL6 cells at the early stage; the second is that Wnt/β-catenin and BMP signaling activity had developmental stage-specific effects on cardiomyogenesis (Fig. 5). Wnt/β-catenin activity at the early stage enhanced embryonic cell differentiation into cardiomyocytes, while suppressing this activity by BMP2 or BMP4 proteins as reported in the avian embryo [26]. In contrast, BMP signaling activity in the late stage enhanced cardiomyocytic differentiation. Grem1 regulated the stage-specific Wnt/β-catenin and BMP signaling activity on cardiomyogenesis.

Many studies have indicated that Grem1 is involved in cell differentiation and development, such as osteogenesis [27], lung morphogenesis [28], myogenesis [29], and limb formation [30], through inhibition of BMP2 and BMP4. Grem1-null mice show intact heart development, despite impairment of lung and kidney [31], and therefore Grem1 is considered not to be involved in cardiogenesis, or supplementary factors such as Noggin [32], with a similar function, may compensate Grem1 during development. Grem1 had an enhancing or promoting activity in *in vitro* cardiomyogenesis, as is the case with platelet-derived growth factor as a promoter of cell growth [33]. In this study, Grem1 was involved in cardiomyocyte differentiation. However Grem1 alone could not induce cardiomyocytic differentiation of CL6 cells in the absence of DMSO (Fig. 2C and F), suggesting that Grem1 is solely

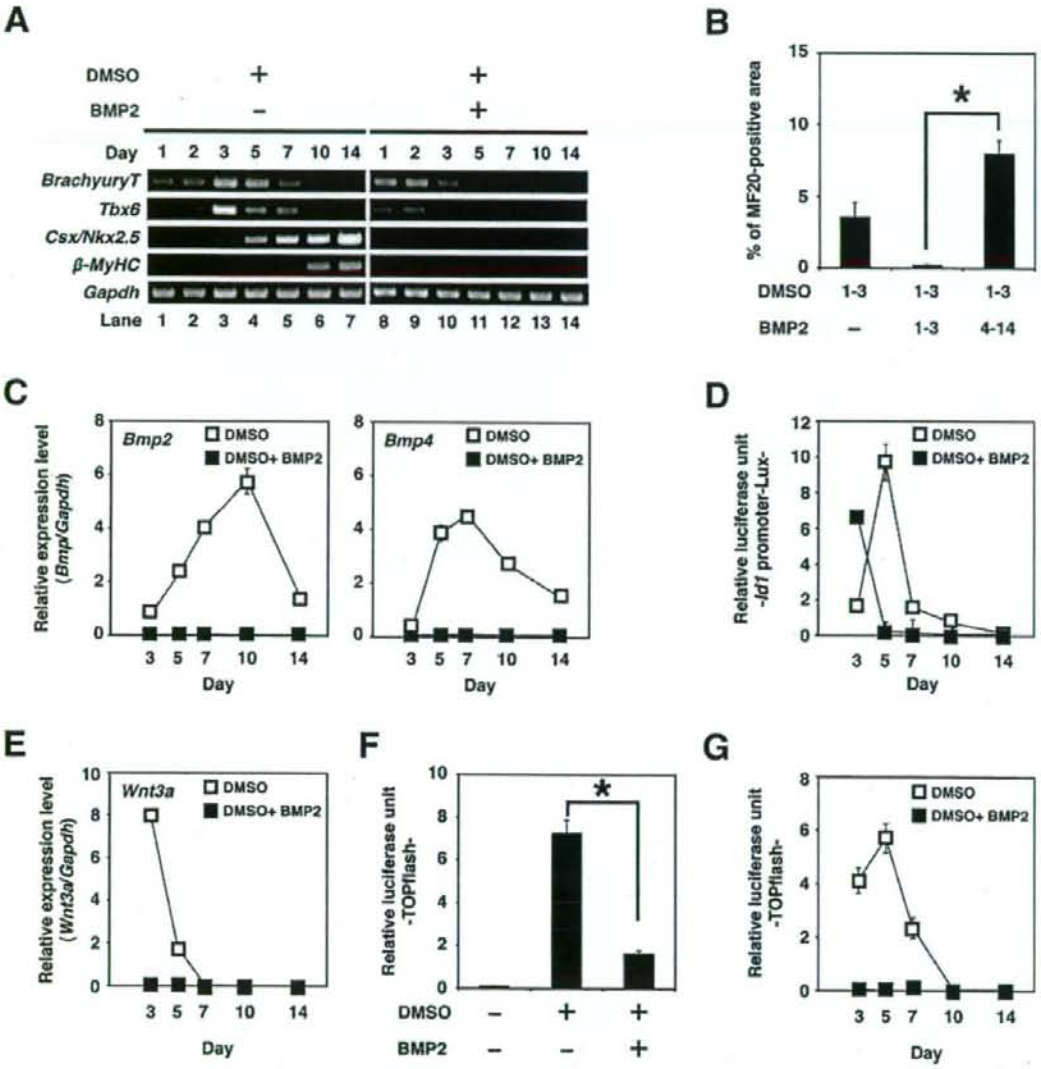


**Figure 4. Cardiomyogenic differentiation in CL6 cells (days 1–3) is inhibited by BMP2.** **(A)** RT-PCR analysis of the gene encoding *BrachyuryT*, *Tbx6*, cardiac-specific transcriptional factor (*Csx/Nkx2.5*), cardiac-specific protein (*β-MyHC*), and *Gapdh* (From top to bottom) of CL6 cells treated with DMSO alone, or DMSO and BMP2 (100 ng/ml) for the first 3 days (days 1–3). The medium, including BMP2 and DMSO, was changed every day. **(B)** Percentage of MF20-positive area. Immunocytochemistry was carried out on CL6 cells 14 days after cells had been exposed to DMSO and BMP2 (100 ng/ml) for the first 3 days (days 1–3). The asterisk indicates a significant statistical difference ($P<0.05$). **(C)** Quantitative real-time RT-PCR analysis of the gene encoding *Bmp2* (left), and *Bmp4* (right) in CL6 cells treated with DMSO alone (open square), or DMSO and BMP2 (100 ng/ml) (closed square) for the first 3 days (days 1–3). **(D)** BMP signaling activity of CL6 cells treated with DMSO alone (open square), or DMSO and BMP2 (100 ng/ml) (closed square) for the first 3 days (days 1–3) were determined by luciferase activity analysis using *Id1* promoter-Lux (a firefly luciferase reporter plasmid driven by the Id1 binding sites), pRL-CMV as co-transfected control, and Dual luciferase reporter assay system. Relative luciferase unit of the CL6 cells untreated with inducers at day 3 is regarded as 0.1 (data not shown). **(E)** Quantitative real-time RT-PCR analysis of the gene encoding *Wnt3a* in CL6 cells treated with DMSO alone (open square), or DMSO and BMP2 (100 ng/ml) (closed square) for the first 3 days (days 1–3). **(F)** Wnt/β-catenin signaling activity of CL6 cells 48 h after exposure to DMSO, or DMSO and BMP2 (100 ng/ml) was determined by luciferase activity analysis using TOPflash (a firefly luciferase reporter plasmid driven by two sets of three copies of the TCF binding site and herpes simple virus thymidine kinase minimal promoter), pRL-CMV as co-transfected control, and Dual luciferase reporter assay system. Relative luciferase unit of the CL6 cells untreated with inducers is regarded as 0.1. The asterisk indicates a significant statistical difference ($P<0.05$). **(G)** Timeframe of Wnt/β-catenin signaling activity in CL6 cells treated with DMSO alone (open square), or DMSO and BMP2 (100 ng/ml) (closed square) for the first 3 days (days 1–3). Relative luciferase unit of the CL6 cells untreated with inducers at day 3 is regarded as 0.1 (data not shown).
doi:10.1371/journal.pone.0002407.g004

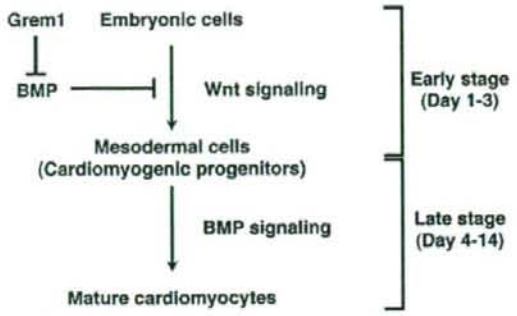


**Figure 5. Grem1-accelerated CL6 cardiomyogenesis through regulation of BMP- and Wnt/β-catenin-signaling pathways.** CL6 embryonic cells start to differentiate into mesodermal cells through Wnt/β-catenin signaling pathway at the early stage (days 1–3), and mesodermal CL6 cells differentiate into mature cardiomyocytes by BMP pathway at the late stage (days 4–14). Grem1 accelerates DMSO-induced cardiomyogenesis through inhibition of the BMP-signaling pathway.
doi:10.1371/journal.pone.0002407.g005

a promoter of cardiomyogenic differentiation. One of the possible mechanisms for Grem1-enhanced cardiomyogenesis at the early stage is inhibition of the BMP signaling pathway [3]. Alternatively, Grem1-enhanced cardiomyogenesis may be mediated through proliferation of cardiac progenitor cells, as is the case of myogenic progenitor proliferation by Grem1 [34], and this possibility is supported by an increased number of sarcomeric myosin-positive CL6 cardiomyocytes (Fig. 2E and F).

The stage specificity of the Grem1 effect is possibly correlated with the biphasic and antagonistic effect of Wnt/β-catenin signaling on cardiomyogenesis, depending on the stage of development *in vitro* [25] and *in vivo* [35]. CL6 cells differentiated into cardiomyocytes via mesodermal induction by the Wnt/β-catenin signaling pathway at the early stage, and CL6 mesodermal cells differentiated into cardiomyocytes induced by BMP2 at the late stage. It is conceivable that embryonic cells, such as CL6 cells and ES cells, differentiate into cardiomyocytes by inhibiting BMP signaling via putative "mesodermal cells" or "cardiomyogenic progenitors", or differentiation stages corresponding to these cells (Fig. 5, Figure S2). The early stage process from embryonic cells to mesodermal cells was mediated via Wnt/β-catenin signaling (Fig. 4F, G), and was assessed by expression of *BrachyuryT* and *Tbx6* genes (Fig. 4A), which are target genes for Wnt/β-catenin signaling [36]. BMP signaling antagonizes the cell fate-inducing activity of Wnt/β-catenin [37]. When embryonic cells or cardiomyogenic progenitors are induced to become mature cardiomyocytes by cytokines and growth factors, we must be careful with respect to the stage of cell differentiation because of the biphasic differential action of the factors which are dependent upon the differentiation stage.

In conclusion, we have demonstrated that Grem1 enhances the commitment or determined path to cardiogenic differentiation of CL6 teratocarcinoma cells. Apart from a role in development, Grem1 may serve a clinical use in cardiology, like granulocyte colony-stimulating factor that accelerates production of granulocytes in both peripheral blood and bone marrow. Nomination of *Grem1* as a cardiomyogenic factor is based on hierarchical clustering analysis using global gene expression data of human cells. This bioinformatics approach may be useful for identifying morphogens/factors that can induce differentiation of other cell types/tissues/organs.

## Materials and Methods

### GeneChip analysis

GeneChip analysis was performed (Fig. 1A, Table 1) as previously described [38]. Human genome-wide gene expression was examined with the Human Genome U133A Probe array (GeneChip; Affymetrix), which contains the oligonucleotide probe set for approximately 23,000 full-length genes and expressed sequence tags, according to the manufacturer's protocol (Expression Analysis technical manual and GeneChip Small Sample Target Labeling Assay version 2 technical note [http://www.affymetrix.com/support/technical/index.affx]). Data analysis was performed by the GeneChip Operation System (Affymetrix) and GeneSpringGX software (Silicon Genetics). To normalize the staining intensity variations between chips, the average difference values for all genes on a given chip were divided by the median of all measurements on that chip. Hierarchical-clustering analysis was performed using a minimum distance value of 0.001, a separation ratio of 0.5, and the standard definition of the correlation distance.

### Cell culture and differentiation

CL6 cells were grown on 100 mm dishes (Becton Dickinson) in α-MEM (Gibco) supplemented with 10% fetal bovine serum (FBS) (JRH Bioscience, Inc.), penicillin, and streptomycin, and were maintained in a 5% $CO_2$ atmosphere at 37°C. To induce differentiation, CL6 cells were plated at a density of $1.8\times10^5$ cells in a 6-well plate (Becton Dickinson) or gelatin-coated 35 mm glass base dishes (IWAKI) with α-MEM containing Grem1 (63 or 125 ng/ml: R&D system) and/or 1% dimethyl sulfoxide (DMSO) for 14 days. Recombinant human bone morphogenetic protein-2 (BMP2) was purchased from R&D systems.

### Reverse transcriptase-PCR (RT-PCR) and quantitative real-time RT-PCR analysis

Total RNAs were extracted from differentiated and undifferentiated CL6 cells and mouse embryonic stem (ES) cells with RNeasy minikit and DNase I treatment (QIAGEN). Mouse ES cell (129 strains) RNA, mouse heart total RNA (Clontech) and mouse skeletal muscle/total RNA (UNITECH. Co., Ltd.) were used as a positive control for each primer. Total RNA (2.0 μg each) for RT-PCR was converted to cDNA with Superscript™ III RNase H– reverse transcriptase (Invitrogen), according to the manufacturer's manual. PCR conditions were optimized and linear amplification range was determined for each primer by varying annealing temperature and cycle number. PCR products were identified by positive control size. RT-PCR was performed using the primers of the genes of cardiac specific transcription factors: *Csx/Nkx2.5*, *Gata4*, *Mef2c*, *Hand2*; circulating hormone: *ANP*, *BNP*; cardiac structural proteins: *β-MyHC*, *MyLC-2a*, *MyLC-2v*; cytokines: *Bmp2*, *Bmp4*, *Fgf8*, *Grem1*, *Wnt1*, *Wnt3a*, *Wnt5a*, *Wnt7a*, *Wnt11*; smooth muscle structural protein: smooth muscle-myosin heavy chain (*SM-MyHC*); the early mesodermal marker: *BrachyuryT*, *T-box6* (*Tbx6*); and *Gapdh* as control. PCR was performed with exTaq DNA polymerase and exTaq PCR buffer (TaKaRa) or LATaq DNA polymerase and GC buffer I (TaKaRa) for 25 or 30 cycles, with each cycle consisting of 95°C for 30 s, 50°C, 55°C, 60°C or 65°C for 45 s, and 72°C for 45 s, with an additional 5 min incubation at 72°C after completion of the final cycle. PCR primers for the genes of *Csx/Nkx2.5*, *Gata4*, *Mef2c*, *Hand2*, *ANP*, *BNP*, *β-MyHC*, *MyLC-2a*, *MyLC-2v*, *Bmp2*, *Bmp4*, *Fgf8*, *Grem1*, *Wnt1*, *Wnt3a*, *Wnt5a*, *Wnt7a*, *Wnt11*, *SM-MyHC*, *BrachyuryT*, *Tbx6*, and *Gapdh* (Table S1a) were obtained from Mouse Genome

Informatics (http://www.informatics.jax.org/). The PCR products were size-fractionated by 2% agarose gel electrophoresis.

Quantitative real-time RT-PCR was performed on an ABI Prism 7700 Sequence Detection System (Applied Biosystems), using 100 ng of cDNA in 25 µl reaction volume with 10 nmol/l of each primer, and 12.5 µl SYBR Green Realtime PCR Master Mix (TOYOBO). PCR primers for the genes of *Bmp2*, *Bmp4*, *Wnt3a*, and *Gapdh* (Table S1b) were obtained from PrimerBank (http://pga.mgh.harvard.edu/primerbank/index.html). Calculations were automatically performed by ABI software (Applied BioSystems).

### Immunocytochemistry

A laser confocal microscope (LSM510, Zeiss) was used for immunocytochemical analysis. Differentiated and undifferentiated CL6 cells were fixed with 4% paraformaldehyde (Wako) for 5 min at 4°C and treated with 0.1% triton X-100 (Sigma) in PBS for 20 min at room temperature, then incubated for 20 min at room temperature in a protein-blocking solution consisting of PBS supplemented with 5% normal goat serum (DakoCytomation). These CL6 cells were then incubated overnight with primary antibody monoclonal anti-sarcomeric myosin antibody (MF20, mouse $IgG_{2b}$ isotype, 1 mg/ml, University of Iowa Hybridoma Bank) and Troponin T, and Cardiac Isoform Ab-1 clone 13-11 (cTnT, mouse $IgG_1$ isotype, 1:300, Lab Vision Corp), or the monoclonal anti-α-actinin (SARCOMERIC) CLONE EA-53 (α-actinin, mouse $IgG_1$ isotype, 1:300, Sigma) in PBS at 4°C. The cells were extensively washed in PBS and incubated at room temperature with Alexa Fluor 568-conjugated goat anti-Mouse $IgG_{2b}$ (anti-MF20) (Molecular Probe; diluted 1:300), Alexa Fluor 488-conjugated goat anti-mouse $IgG_1$ (anti-cTnT) (Molecular Probe; diluted 1:300), Alexa Fluor 546-conjugated goat anti-mouse IgG(H+L) (anti-α-actinin) (Molecular Probe; diluted 1:300), and nuclei were counterstained with 4', 6-diamidino-2-phenylindole (DAPI) (Wako; diluted 1:300) for 45 min. To prevent fading, cells were then mounted in DakoCytomation Fluorescent Mounting Medium (DakoCytomation).

### Transfection and luciferase assays

Cells ($8.0\times10^5$) seeded and cultured in 60 mm dishes (Becton Dickinson) were transfected 18 h after plating using Lipofectamine 2000 (Invitrogen) and PLUS reagent (Invitrogen) in Opti-MEM (Gibco). Transfection contained 1.0 µg of TOPflash plasmid (Upstate Biotechnology) for measurement of Wnt/β-catenin activity, or 5.0 µg of the *Id1* promoter-Lux plasmid (provided by Dr Imamura and Dr Miyazono) for measurement of BMP-induced *Id1* gene transcription, and 0.5 µg of pRL-CMV (Promega) as co-transfected control. Medium containing 10% FBS was changed 3 h after transfection and transfected cells ($1.8\times10^5$) were re-seeded in 6-well plates 24 h after transfection. After 18 h, CL6 cells were induced with BMP2 (100 ng/ml) and DMSO. CL6 cells were prepared for luciferase activity analysis using Dual luciferase reporter assay system (Promega).

### Area calculation

The regions of interest (beating area, immunostaining area) were defined in Photoshop (Adobe systems) using the 'magic wand' tool. The total numbers of pixels identified were then counted using the histogram function. At least five different fields were measured for each dish.

### Statistical analysis

Results, shown as the mean±SE, were compared by ANOVA followed by Scheffé's test, with $P<0.05$ considered significant.

## Supporting Information

**Figure S1** A semi-quantitative RT-PCR of cardiomyocyte-specific genes. To investigate expression level of cardiomyocyte-specific genes (Csx/Nkx2.5, Gata4, MyLC-2a, and MyLC-2v), a semi-quantitative RT-PCR was performed from CL6 cells treated with 1% DMSO and the indicated concentration of Grem1 for 14 days. Each RT-PCR product was electrophoresed in 2% agarose gel, and was measured using ImageJ software (http://rsb.info.nih.gov/ij/) to calculate the ratio of each gene to Gapdh. The expression level for each gene is determined relative to that of Gapdh, and expression level in CL6 cells treated with DMSO alone was regarded as 1.0. The relative expression levels were averaged from at least three independent experiments.
Found at: doi:10.1371/journal.pone.0002407.s001 (1.04 MB DOC)

**Figure S2** Grem1 enhanced cardiomyogenic differentiation of mouse ES cells. Mouse ES cells (NCH1.5, C57BL/6J×129ter/Sv) were cultured on a mouse embryonic fibroblast feeder layer inactivated with 30 Gy γ-irradiation in gelatin-coated 60 mm dishes (Becton, Dickinson). Cells were grown in KnockOut DMEM (Gibco) supplemented with 15% fetal bovine serum (Cell Culture Technologies), 2 mM GlutaMAX (Gibco), 0.1 mM non-essential amino acid (Gibco), 0.1 mM 2-mercaptoethanol (Gibco), penicillin, streptomycin, and 2,000 U/ml mouse leukemia inhibitory factor (LIF) (Chemicon). For cardiomyogenic differentiation, ES cells were exposed to 125 ng/ml Grem1 (R&D systems) for the three days. The cells were then trypsinized and cultured to form embryonic bodies (EBs) from a single cell using a three-dimensional culture system (without LIF) on low cell binding dishes (96-well plate round bottom). This represented day 0 of EB formation. On the next day, the medium was replaced with the same medium without LIF. EBs were re-seeded on gelatin-coated 48-well plates with one EB per well, on day 8 after the start of EB formation. The cardiomyogenic induction was estimated by the beating EB number per total EB number, measured on day 12 under a phase-contrast microscope. Grem1 increased the percentage of beating EBs to 69.2%, as compared with 26.7% in EBs without Grem1 treatment. The numbers in parentheses indicate the EB numbers counted.
Found at: doi:10.1371/journal.pone.0002407.s002 (1.27 MB DOC)

**Table S1** Primer sequences.
Found at: doi:10.1371/journal.pone.0002407.s003 (0.06 MB DOC)

**Movie S1** CL6 cells treated with DMSO alone. P19CL6 cells are reproducibly and stably induced into beating cardiomyocytes with DMSO.
Found at: doi:10.1371/journal.pone.0002407.s004 (1.66 MB MOV)

**Movie S2** CL6 cells treated with Grem1 (125 ng/ml) and DMSO. Grem1 dramatically promotes DMSO-induced cardiomyogenic differentiation of P19CL6 cells at a concentration of 125 ng/ml.
Found at: doi:10.1371/journal.pone.0002407.s005 (2.40 MB MOV)

## Acknowledgments

We would like to express our sincere thanks to T. Imamura and K. Miyazono for the *Id1* promoter-Lux plasmid, and J. Fujimoto for their discussion of this work.

## Author Contributions

Conceived and designed the experiments: AU DK. Performed the experiments: DK HM RI KM. Analyzed the data: AU AN DK YT RI MT MW. Contributed reagents/materials/analysis tools: IK AN IS HS. Wrote the paper: AU DK.

## References


1. Andree B, Duprez D, Vorbusch B, Arnold HH, Brand T (1998) BMP-2 induces ectopic expression of cardiac lineage markers and interferes with somite formation in chicken embryos. Mech Dev 70: 119–131.
2. Schultheiss TM, Burch JB, Lassar AB (1997) A role for bone morphogenetic proteins in the induction of cardiac myogenesis. Genes Dev 11: 451–462.
3. Angello JC, Kaestner S, Welikson RE, Buskin JN, Hauschka SD (2006) BMP induction of cardiogenesis in P19 cells requires prior cell-cell interaction(s). Dev Dyn 235: 2122–2133.
4. Alsan BH, Schultheiss TM (2002) Regulation of avian cardiogenesis by Fgf8 signaling. Development 129: 1935–1943.
5. Crossley PH, Martin GR (1995) The mouse Fgf8 gene encodes a family of polypeptides and is expressed in regions that direct outgrowth and patterning in the developing embryo. Development 121: 439–451.
6. Reifers F, Walsh EC, Leger S, Stainier DY, Brand M (2000) Induction and differentiation of the zebrafish heart requires fibroblast growth factor 8 (fgf8/acerebellar). Development 127: 225–235.
7. Whitehead GG, Makino S, Lien CL, Keating MT (2005) fgf20 is essential for initiating zebrafish fin regeneration. Science 310: 1957–1960.
8. Yamagishi H, Olson EN, Srivastava D (2000) The basic helix-loop-helix transcription factor, dHAND, is required for vascular development. J Clin Invest 105: 261–270.
9. Ariizumi T, Kinoshita M, Yokota C, Takano K, Fukuda K, et al. (2003) Amphibian in vitro heart induction: a simple and reliable model for the study of vertebrate cardiac development. Int J Dev Biol 47: 405–410.
10. Gavert N, Ben-Ze'ev A (2007) beta-Catenin signaling in biological control and cancer. J Cell Biochem 102: 820–828.
11. Chien KR, Moretti A, Laugwitz KL (2004) Development. ES cells to the rescue. Science 306: 239–240.
12. Pandur P, Lasche M, Eisenberg LM, Kuhl M (2002) Wnt-11 activation of a non-canonical Wnt signalling pathway is required for cardiogenesis. Nature 418: 636–641.
13. Yamagishi H, Yamagishi C, Nakagawa O, Harvey RP, Olson EN, et al. (2001) The combinatorial activities of Nkx2.5 and dHAND are essential for cardiac ventricle formation. Dev Biol 239: 190–203.
14. Park M, Wu X, Golden K, Axelrod JD, Bodmer R (1996) The wingless signaling pathway is directly involved in Drosophila heart development. Dev Biol 177: 104–116.
15. Marvin MJ, Di Rocco G, Gardiner A, Bush SM, Lassar AB (2001) Inhibition of Wnt activity induces heart formation from posterior mesoderm. Genes Dev 15: 316–327.
16. Schneider VA, Mercola M (2001) Wnt antagonism initiates cardiogenesis in Xenopus laevis. Genes Dev 15: 304–315.
17. Tzahor E, Lassar AB (2001) Wnt signals from the neural tube block ectopic cardiogenesis. Genes Dev 15: 255–260.
18. Olson EN (2001) Development. The path to the heart and the road not taken. Science 291: 2327–2328.
19. Terami H, Hidaka K, Katsumata T, Iio A, Morisaki T (2004) Wnt11 facilitates embryonic stem cell differentiation to Nkx2.5-positive cardiomyocytes. Biochem Biophys Res Commun 325: 968–975.
20. Sharov AA, Dudekula DB, Ko MS (2005) A web-based tool for principal component and significance analysis of microarray data. Bioinformatics 21: 2548–2549.
21. Hamatani T, Carter MG, Sharov AA, Ko MS (2004) Dynamics of global gene expression changes during mouse preimplantation development. Dev Cell 6: 117–131.
22. Sharov AA, Dudekula DB, Ko MSH (2005) http://lgsun.grc.nia.nih.gov/ANOVA/help.html#hierarchical Accessed 2007 April 20. Bioinformatics Advance Access.
23. Naito AT, Akazawa H, Takano H, Minamino T, Nagai T, et al. (2005) Phosphatidylinositol 3-kinase-Akt pathway plays a critical role in early cardiomyogenesis by regulating canonical Wnt signaling. Circ Res 97: 144–151.
24. Hsu DR, Economides AN, Wang X, Eimon PM, Harland RM (1998) The Xenopus dorsalizing factor Gremlin identifies a novel family of secreted proteins that antagonize BMP activities. Mol Cell 1: 673–683.
25. Naito AT, Shiojima I, Akazawa H, Hidaka K, Morisaki T, et al. (2006) Developmental stage-specific biphasic roles of Wnt/beta-catenin signaling in cardiomyogenesis and hematopoiesis. Proc Natl Acad Sci U S A 103: 19812–19817.
26. Jin EJ, Erickson CA, Takada S, Burrus LW (2001) Wnt and BMP signaling govern lineage segregation of melanocytes in the avian embryo. Dev Biol 233: 22–37.
27. Sutherland MK, Geoghegan JC, Yu C, Turcott E, Skonier JE, et al. (2004) Sclerostin promotes the apoptosis of human osteoblastic cells: a novel regulation of bone formation. Bone 35: 828–835.
28. Shi W, Zhao J, Anderson KD, Warburton D (2001) Gremlin negatively modulates BMP-4 induction of embryonic mouse lung branching morphogenesis. Am J Physiol Lung Cell Mol Physiol 280: L1030–1039.
29. Tzahor E, Kempf H, Mootoosamy RC, Poon AC, Abzhanov A, et al. (2003) Antagonists of Wnt and BMP signaling promote the formation of vertebrate head muscle. Genes Dev 17: 3087–3099.
30. Zuniga A, Michos O, Spitz F, Haramis AP, Panman L, et al. (2004) Mouse limb deformity mutations disrupt a global control region within the large regulatory landscape required for Gremlin expression. Genes Dev 18: 1553–1564.
31. Michos O, Panman L, Vintersten K, Beier K, Zeller R, et al. (2004) Gremlin-mediated BMP antagonism induces the epithelial-mesenchymal feedback signaling controlling metanephric kidney and limb organogenesis. Development 131: 3401–3410.
32. Yuasa S, Itabashi Y, Koshimizu U, Tanaka T, Sugimura K, et al. (2005) Transient inhibition of BMP signaling by Noggin induces cardiomyocyte differentiation of mouse embryonic stem cells. Nat Biotechnol 23: 607–611.
33. Singh JP, Chaikin MA, Pledger WJ, Scher CD, Stiles CD (1983) Persistence of the mitogenic response to platelet-derived growth factor (competence) does not reflect a long-term interaction between the growth factor and the target cell. J Cell Biol 96: 1497–1502.
34. Frank NY, Kho AT, Schatton T, Murphy GF, Molloy MJ, et al. (2006) Regulation of myogenic progenitor proliferation in human fetal skeletal muscle by BMP4 and its antagonist Gremlin. J Cell Biol 175: 99–110.
35. Klaus A, Saga Y, Taketo MM, Tzahor E, Birchmeier W (2007) Distinct roles of Wnt/beta-catenin and Bmp signaling during early cardiogenesis. Proc Natl Acad Sci U S A 104: 18531–18536.
36. Yamaguchi TP, Takada S, Yoshikawa Y, Wu N, McMahon AP (1999) T (Brachyury) is a direct target of Wnt3a during paraxial mesoderm specification. Genes Dev 13: 3185–3190.
37. Kleber M, Lee HY, Wurdak H, Buchstaller J, Riccomagno MM, et al. (2005) Neural crest stem cell maintenance by combinatorial Wnt and BMP signaling. J Cell Biol 169: 309–320.
38. Sugiki T, Uyama T, Toyoda M, Morioka H, Kume S, et al. (2007) Hyaline cartilage formation and enchondral ossification modeled with KUM5 and OP9 chondroblasts. J Cell Biochem 100: 1240–1254.

OPEN ACCESS Freely available online PLoS one

# Nicotine Acts on Growth Plate Chondrocytes to Delay Skeletal Growth through the α7 Neuronal Nicotinic Acetylcholine Receptor

**Atsuo Kawakita[1,2], Kazuki Sato[2], Hatsune Makino[1], Hiroyasu Ikegami[2], Shinichiro Takayama[3], Yoshiaki Toyama[2], Akihiro Umezawa[1]***

**1** Department of Reproductive Biology, National Institute for Child Health and Development, Tokyo, Japan, **2** Department of Orthopaedic Surgery, Keio University School of Medicine, Tokyo, Japan, **3** Department of Orthopaedic Surgery, National Center for Child Health and Development, Tokyo, Japan

## Abstract

***Background:*** Cigarette smoking adversely affects endochondral ossification during the course of skeletal growth. Among a plethora of cigarette chemicals, nicotine is one of the primary candidate compounds responsible for the cause of smoking-induced delayed skeletal growth. However, the possible mechanism of delayed skeletal growth caused by nicotine remains unclarified. In the last decade, localization of neuronal nicotinic acetylcholine receptor (nAChR), a specific receptor of nicotine, has been widely detected in non-excitable cells. Therefore, we hypothesized that nicotine affect growth plate chondrocytes directly and specifically through nAChR to delay skeletal growth.

***Methodology/Principal Findings:*** We investigated the effect of nicotine on human growth plate chondrocytes, a major component of endochondral ossification. The chondrocytes were derived from extra human fingers. Nicotine inhibited matrix synthesis and hypertrophic differentiation in human growth plate chondrocytes in suspension culture in a concentration-dependent manner. Both human and murine growth plate chondrocytes expressed alpha7 nAChR, which constitutes functional homopentameric receptors. Methyllycaconitine (MLA), a specific antagonist of alpha7 nAChR, reversed the inhibition of matrix synthesis and functional calcium signal by nicotine in human growth plate chondrocytes in vitro. To study the effect of nicotine on growth plate in vivo, ovulation-controlled pregnant alpha7 nAChR +/− mice were given drinking water with or without nicotine during pregnancy, and skeletal growth of their fetuses was observed. Maternal nicotine exposure resulted in delayed skeletal growth of alpha7 nAChR +/+ fetuses but not in alpha7 nAChR −/− fetuses, implying that skeletal growth retardation by nicotine is specifically mediated via fetal alpha7 nAChR.

***Conclusions/Significance:*** These results suggest that nicotine, from cigarette smoking, acts directly on growth plate chondrocytes to decrease matrix synthesis, suppress hypertrophic differentiation via alpha7 nAChR, leading to delayed skeletal growth.

**Citation:** Kawakita A, Sato K, Makino H, Ikegami H, Takayama S, et al. (2008) Nicotine Acts on Growth Plate Chondrocytes to Delay Skeletal Growth through the α7 Neuronal Nicotinic Acetylcholine Receptor. PLoS ONE 3(12): e3945. doi:10.1371/journal.pone.0003945

**Editor:** Rory Edward Morty, University of Giessen Lung Center, Germany

**Received** August 6, 2008; **Accepted** November 8, 2008; **Published** December 16, 2008



**Funding:** This study was supported by a grant from the Smoking Research Foundation; by grants from the Ministry of Education, Culture, Sports, Science, and Technology (MEXT) of Japan; by the Ministry of Health, Labour and Welfare (MHLW) Sciences Research Grants; by a Research Grant on Health Science focusing on Drug Innovation from the Japan Health Science Foundation; by the program for promotion of Fundamental Studies in Health Science of the Pharmaceuticals and Medical Devices Agency; by a Research Grant for Cardiovascular Disease from the MHLW; and by a Grant for Child Health and Development from the MHLW. The funders had no role in study design, data collection and analysis, decision to publish, or preparation of the manuscript.

**Competing Interests:** The authors have declared that no competing interests exist.

* E-mail: umezawa@1985.jukuin.keio.ac.jp

## Introduction

Though detrimental effects of cigarette smoking to the human body have been widely demonstrated, the effects on endochondral ossification are not well understood. Epidemiologically, maternal smoking reduces the height of newborns [1–5]. However, there are controversial views regarding the mechanisms behind delayed skeletal growth caused by cigarette smoking. The socioeconomic status of smoking mothers [6,7], deficient maternal diet [8], chronic hypoxia caused by carbon monoxide [9], impaired placental size and function, and decreased blood flow of placenta caused by nicotine [10] have all been reported as a possible causal factors responsible for reduction in height of newborns. Conversely, it has also been reported that socioeconomic status [11], maternal diet [12], and hypoxia are not responsible for the cause of delayed skeletal growth. Research suggests that smoking not only reduces body length but also brings ossification retardation in the rat smoking model [13]. Moreover, smoking delays chondrogenesis in a mouse model of fracture healing [14]. Cigarette smoking, thus, adversely affects endochondral ossification somehow during the course of skeletal growth and repair in animal models.

Among a multitude of chemicals and physiological functions arising from cigarette smoking, nicotine is one of the leading candidates for causing small newborns. Epidemiologically, nicotine content in cigarette is related to reduced birth length in humans [15]. However, the possible mechanism of delayed skeletal growth caused by nicotine remains unclarified. In this study, we investigated the effect of nicotine on growth plate chondrocytes, the principle

component of endochondral ossification. In the last decade, localization of neuronal nicotinic acetylcholine receptor (nAChR), a specific receptor of nicotine, has been widely detected in non-excitable cells [16]. Therefore, we hypothesized that nicotine affect growth plate chondrocytes directly and specifically through nAChR to delay skeletal growth. We here demonstrate that nicotine affected growth plate chondrocytes through alpha7 nAChR to decrease matrix synthesis and to suppress hypertrophic differentiation, thereby delaying skeletal growth.

## Results

### Detection and localization of nAChR in growth plate chondrocytes

To date, many epidemiological [1–5] and experimental [13] studies suggested that endochondral ossification is affected by cigarette smoking, especially by its major component, nicotine [15]. We thus assumed that nicotine may directly affect chondrocytes, a key player in endochondral ossification. To investigate whether the impact of nicotine on chondrocytes is specific, we studied the expression pattern of the specific receptor, nAChR. For screening of the existing subunits of nAChR, RT-PCR was performed with primers for each subunit of nAChR. Human growth plate chondrocytes expressed alpha5, alpha7, beta1 and epsilon subunits of nAChR (Figure 1A).

Among the detected subunits, only the alpha7 subunit can form a functional nAChR by forming a homopentameric receptor [17]. We thus tried to detect alpha7 subunit at a protein level. Western blot analysis revealed that chondrocytes produced alpha7 nAChR (Figure 1B). Immunocytochemical analysis also revealed that chondrocytes stained positive for alpha7 nAChR (Figure 1C). Moreover, the alpha7 subunit was detected at resting, proliferating and pre-hypertrophic chondrocytes of murine growth plate but not hypertrophic chondrocytes (Figure 1D). These results suggest that the growth plate chondrocytes in their non-hypertrophic stage express alpha7 homopentameric nAChR.

### Effect of nicotine on chondrocytes cultured in agarose gel

To study the effect of nicotine on growth plate chondrocytes in vitro, two methods of suspension cultures, i.e., agarose gel culture and alginate bead culture, were employed. In agarose gel, the chondrocytes are initially embedded in the suspension layer solitarily. The chondrocytes then proliferate, differentiate, and aggregate to form a colony in the presence of ascorbic acid, and start to produce a matrix around themselves [18]. We applied the agarose gel culture to study the effect of nicotine on the proliferation and differentiation of growth plate chondrocytes in vitro. Nicotine was added to culture media for three weeks culture period. Nicotine decreased the percentage of colonies which produce matrix, as revealed by alcian blue (ALB) stains in a concentration-dependent manner (Figure 2A, upper panels). Similarly, nicotine suppressed Col X expression and enzyme activity of alkaline phosphatase (ALP) in a concentration-dependent manner (Figure 2A, middle and lower row panels). In contrast, nicotine did not affect colony density (Figure 2B, left panel) or the number of cells per colony (Figure 2B, right panel) which are indicators for cell proliferation. No nicotinic effect on cell proliferation was detected as assessed by immunohistochemistry using antibody to proliferating cell nuclear antigen (PCNA) (Figure S1). These results suggest that nicotine decreases the matrix synthesis and suppresses hypertrophic differentiation of growth plate chondrocytes, but has little effect on cell proliferation in vitro and vivo. To investigate if the nicotinic effect is mediated by alpha7 nAChR, we used MLA, the specific antagonist of alpha7 nAChR. MLA clearly reversed the effect, as assessed by ALB-stained colonies (Figure 2C), suggesting the involvement of alpha7 nAChR in the effect of nicotine on growth plate chondrocytes.

### Long-term (four months) effect of nicotine on growth plate chondrocytes in alginate beads

Different from the case with agarose gel, human chondrocytes hardly proliferate in alginate beads, maintaining chondrocyte properties for more than eight months [19]. Moreover, molecular analysis can be done easily compared with that in agarose gel, since chondrocytes can be recovered from beads by chelation of divalent ions with ethylenediamine tetraacetic acid (EDTA) followed by centrifugation. We investigated the long-term effect of nicotine on growth plate chondrocytes by employing alginate bead culture. Chondrocytes encapsulated in alginate beads remained viable during the culture period (four months) in their lacunae. Nicotine did not affect viability of the chondrocytes at any indicated concentration. Nicotine dose-dependently suppressed ALB- and Safranin-O-stained areas at four months (Figure 3A).

To investigate expression of chondrocyte-specific genes, we performed RT-PCR analysis on chondrocytes in alginate beads. Genes for collagen type II (Col II), Aggrecan, collagen type X (ColX), ALP, and indian hedgehog (Ihh) were up-regulated at three weeks after the start of alginate bead culture (Figure 3B). In contrast, genes for parathyroid hormone receptor type I (PTHR1), matrix metalloproteinase type 13 (MMP13), vascular endothelial growth factor (VEGF), and Sox9 were constitutionally expressed and their expression level remained unchanged. We then performed RT-PCR analysis to investigate the expression of chondrocyte-specific genes in chondrocytes treated by nicotine for four months. Nicotine dose-dependently decreased the expression of Col II, Aggrecan, Col X, ALP, and Ihh gene (Figure 3C). These findings suggest that nicotine suppresses matrix synthesis and hypertrophic maturation of chondrocytes in long-term culture using alginate beads.

### Functional calcium imaging

To investigate the intracellular signals after nicotinic stimulation, we performed calcium imaging assay for primary chondrocyte cultures, since alpha7 nAChR has large $Ca^{2+}$ permeabilities and also induces elevated intracellular free calcium by releasing intracellular calcium stores [17]. Nicotine elicited a transient increase of intra-cellular calcium (Figure 4A) in a concentration-dependent manner (Figure 4B). MLA, the specific antagonist of alpha7 nAChR, inhibited the calcium signals in a concentration-dependent manner (Figure 4C), implying that the effect of nicotine on chondrocytes is mediated through the alpha7 nAChR.

### Maternal nicotine exposure in wild-type mice

To study the effect of nicotine on endochondral ossification in vivo, ovulation-controlled pregnant C57BL/6J mice were given drinking water with or without nicotine during pregnancy, and skeletal growth of their fetuses was observed. At noon on gestational day 15, fetuses were surgicallly obtained and their legs were sectioned for measurement of the femur length (FL) and the length of the hypertrophic zone of the femur (HL) (Figure 5A). There were no significant differences of the amount of water consumed between nicotine-exposed group and control group. Maternal nicotine exposure significantly reduced the FL (Figure 5B) and HL/FL (Figure 5C) of mice at embryonic day 15.5 (E15.5), suggesting that nicotine delayed endochondral ossification.

### Maternal nicotine exposure in alpha7 nAChR-disrupted mice

To clarify an involvement of alpha7 nAChR in nicotine-induced delayed skeletal growth in vivo, we investigated the effect

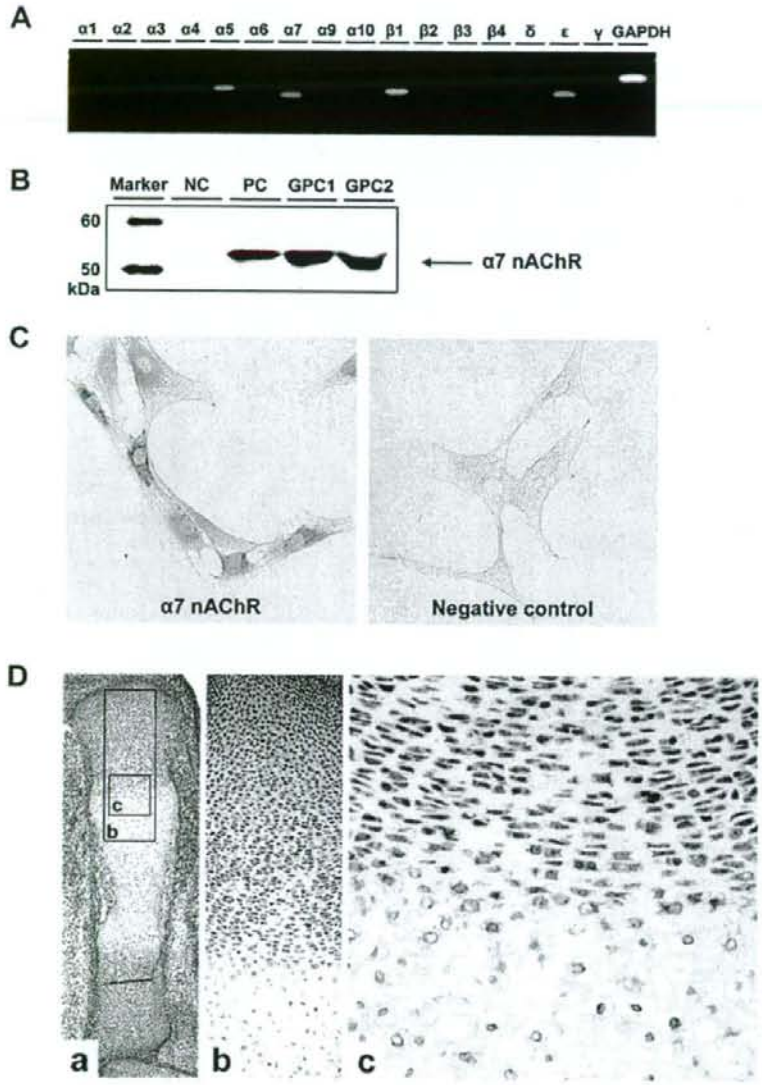


**Figure 1. Detection and localization of nAChR subunits in growth plate chondrocytes.** A: The expression of each subunit of nAChR. Total RNA was isolated from primary culture of human growth plate chondrocytes. The primers for each subunit are listed in Tables S1–S3. RT-PCR amplified products of alpha5, alpha7, beta1 and epsilon subunits of nAChR and GAPDH. B: Western blot analysis of alpha7 subunit of nAChR in primary chondrocyte cultures. NC: negative control (adipocyte), PC: positive control (PC-12 cell), GPC1,2: human growth plate chondrocyte derived from extra fingers of two individuals. C: Immunocytochemical analysis of alpha7 nAChR subunit in human growth plate chondrocytes. Primary chondrocytes were stained with alpha7 nAChR subunit-specific antibody. D: Immunohistochemical analysis of alpha7 nAChR subunit in tibia of E15.5 fetuses. Alpha7 nAChR are detected at resting, proliferating and pre-hypertrophic chondrocytes of murine growth plate.
doi:10.1371/journal.pone.0003945.g001

of maternal nicotine exposure on skeletal development of murine fetuses in which the alpha7 nAChR gene is disrupted. Maternal genotype is alpha7 nAChR +/− in this experiment (Figure 6), unlike the experiment using wild type mice (Figure 5, maternal genotype: alpha7 nAChR +/+), and littermate fetuses (alpha7 nAChR −/− and alpha7 nAChR +/+) were compared to exclude the effect of nicotine on maternal bodies. Nicotine significantly reduced FL and HL/FL in alpha7 nAChR +/+ fetuses but not in alpha7 nAChR −/− fetuses (Figure 6A, B). However, nicotine did not significantly affect body weight (BW) in both genotypes

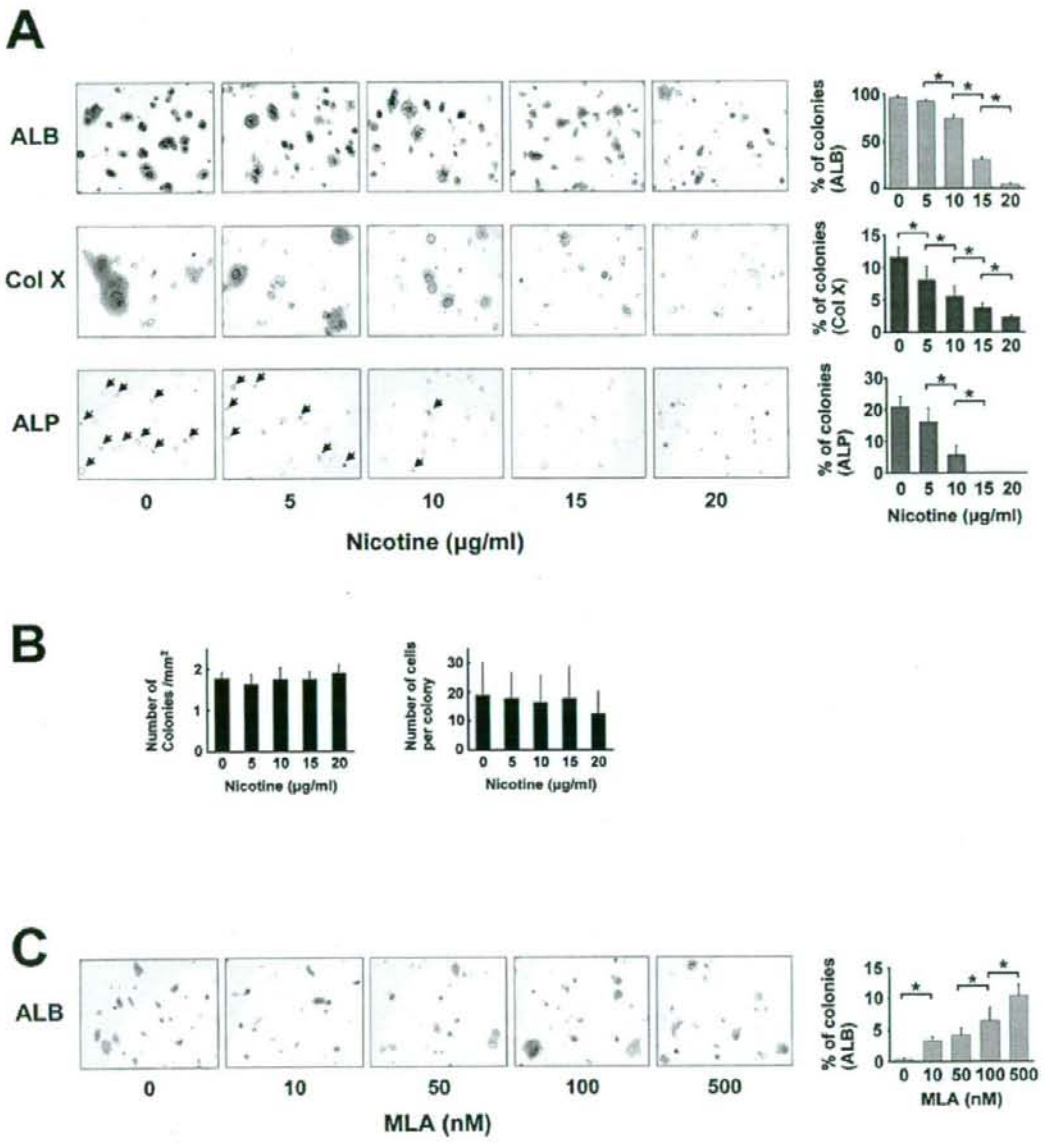


**Figure 2. Effect of nicotine on growth plate chondrocytes in agarose gel.** Growth plate chondrocytes were cultured in an agarose gel using the modified method previously described [28], and exposed to nicotine and MLA, a specific antagonist for alpha7 nAChR, at the indicated concentration. After three weeks of cultivation, suspension agarose was transferred to a glass slide and the following histological analyses were then performed. A: Microscopic appearance of chondrocyte colonies. From top to bottom: ALB (Alcian blue stain), Col X (immunocytochemistry by an anti-Col X antibody), ALP (enzyme cytochemistry of alkaline phosphatase). For ALB and Col X stain, the slides were counterstained with kernechtrot and hematoxylin, respectively. Percentage of ALB- stained, Col X- positive, and Alkaline phosphatase- positive colonies were counted (right panel, from top to bottom). All the ALP positive colonies in the panels are indicated by arrowheads. Nicotine concentration-dependently suppressed the percentage of the colonies stained with ALB, Col X, and ALP. *, statistically significant, $P<0.02$. B: Number of colonies and number of cells per colony. The number of colonies with a diameter greater than 50 μm (left panel) and cell number per colony (right panel) were counted on the ALB- stained agarose gel slides. C: Microscopic appearance of chondrocyte colonies stained with ALB. MLA reversed the decrease of ALB- positive matrix in a concentration-dependent manner under constant nicotine concentration (20 μg/ml). The percentage of ALB-positive colonies exceeded 10% by using 500 nM MLA. *, statistically significant, $P<0.02$.

doi:10.1371/journal.pone.0003945.g002

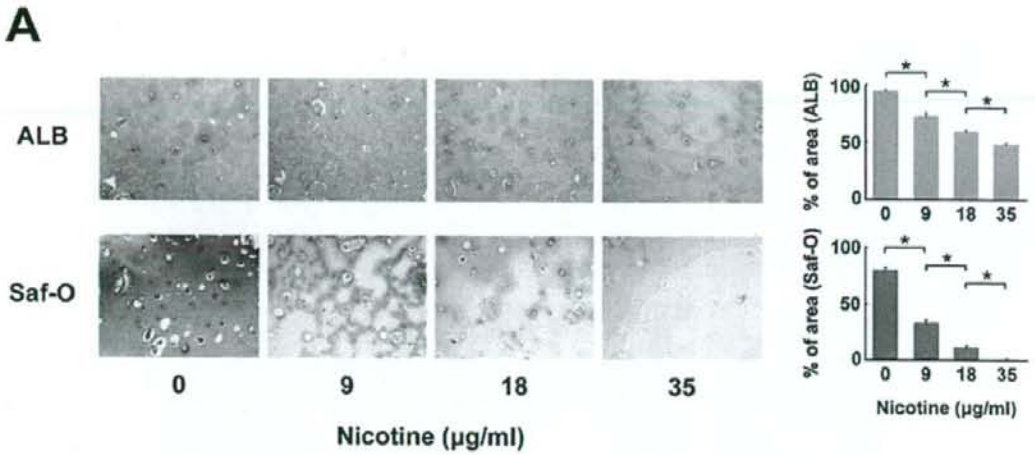


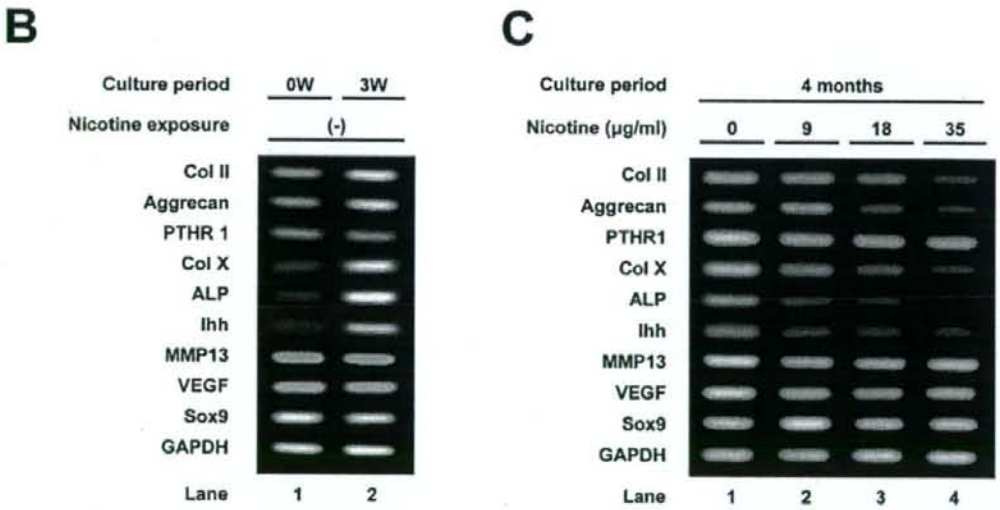


**Figure 3. Long-term (four months) effect of nicotine on growth plate chondrocytes in alginate beads.** Growth plate chondrocytes in alginate beads were exposed to the indicated concentration of nicotine for four months. A: Microscopic view of chondrocytes in alginate beads after four-months cultivation. Upper panels: ALB stain, lower panels: Safranin-O stain. Chondrocytes were surrounded by matrix which they secreted. Nicotine decreased the area stained with ALB or Safranin-O in a concentration-dependent manner. *, statistically significant, $P<0.02$. B: RT-PCR analysis of chondrocyte-specific gene expression in the chondrocytes at the start of cultivation (lane 1: 0W) and three weeks (lane 2: 3W). From top to bottom: genes for Col II, Aggrecan, parathyroid hormone receptor type 1 (PTHR1), Col X, alkaline phosphatase (ALP), Indian hedgehog (Ihh), matrix metalloproteinase type13 (MMP13), vascular endothelial growth factor (VEGF), Sox9 and GAPDH. C: RT-PCR analysis of chondrocyte-specific gene expression in chondrocytes embedded in alginate beads exposed to the indicated concentration of nicotine for four months. Expression of early stage matrix-gene (Col II and Aggrecan) and markers of hypertrophic chondrocytes (Col X, ALP and Ihh) increased after three weeks of cultivation (B). Nicotine decreased the expression of these genes in a concentration-dependent manner, but had little effect for the expression of MMP13, VEGF, and control genes (Sox9 and GAPDH) (C).
doi:10.1371/journal.pone.0003945.g003

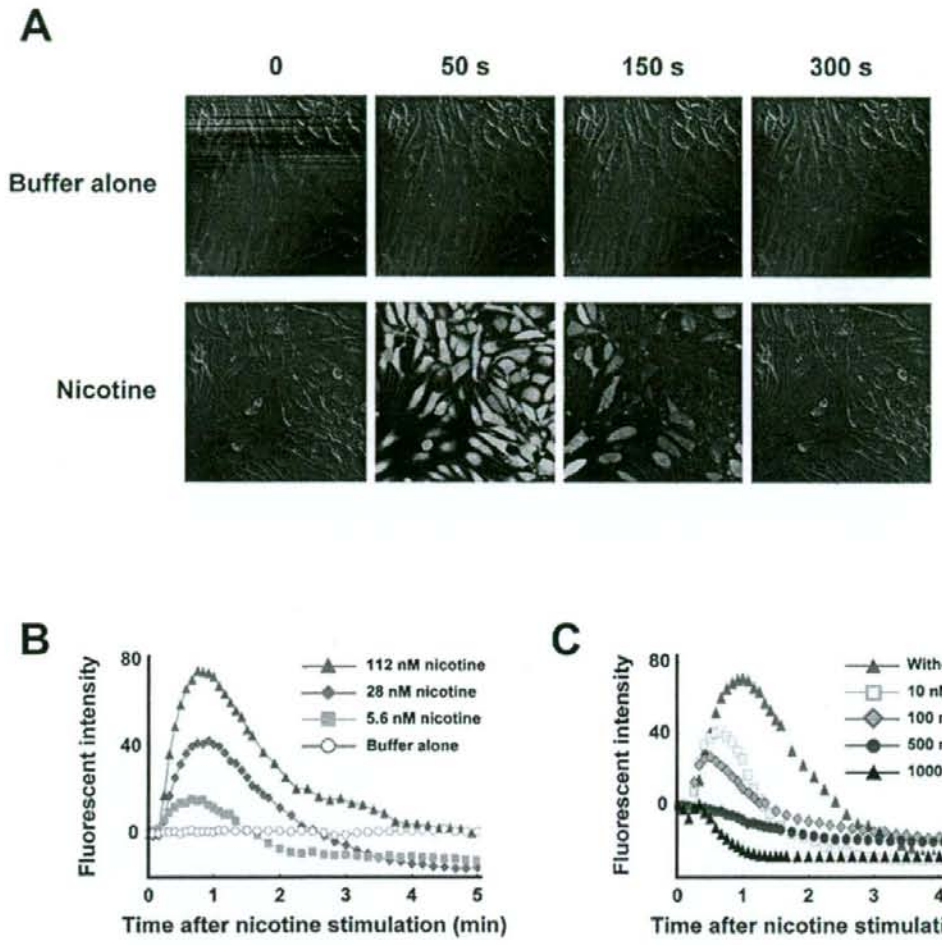


**Figure 4. Calcium influx assay in primary chondrocyte culture.** Nicotine-stimulated calcium signaling was investigated by the use of a fluorescent $Ca^{2+}$ indicator. Primary chondrocyte cultures were stimulated by nicotine with or without MLA, the specific antagonist of alpha7 homomeric nAChR. A: Addition of assay buffer alone elicits no reaction (upper panels: negative control). Nicotine elicits a transient increase of intracellular calcium (lower panels). B: Nicotine elicits a transient increase of intra-cellular calcium in a concentration-dependent manner. C: MLA inhibits nicotine-induced calcium influx in a concentration-dependent manner. The cells were treated with MLA 30 min before nicotine stimulation.
doi:10.1371/journal.pone.0003945.g004

(Figure 6C). Besides, scatterplot and correlation between the FL and the BW revealed that nicotine downwardly shifted the linear slope in alpha7 nAChR +/+ fetuses but had no effect in alpha7 nAChR −/− fetuses (Figure 6D). These findings suggest that maternal nicotine exposure decreased the fetal endochondral ossification through the fetal alpha7 nAChR in vivo.

## Discussion

Alpha7 nAChR was originally identified as a subunit of neuronal nAChR, and has also been shown to be functional in both neuronal and non-neuronal, i.e., non-excitable cells such as lymphocytes, vascular endothelial cells, keratinocytes and bronchial epithelium [16]. In this study, we demonstrated the expression of the alpha7 subunit of nAChR at resting to pre-hypertrophic chondrocytes in murine growth plate and on a culture of human growth plate chondrocytes, and the involvement of alpha7 nAChR in nicotine-induced delayed skeletal growth. The novel findings of alpha7 nAChR in chondrocytes suggest that the effect of smoking on delayed skeletal growth is directly correlated with nicotinic action on chondrocytes.

### Direct effect of nicotine on human growth plate chondrocytes

Maternal nicotine exposure decreases the width of the hypertrophic zone of growth plate, increases apoptotic chondrocytes, and reduces the length of femur in rat [20]. Contrarily, nicotine has been shown to up-regulate glycosaminoglycan and

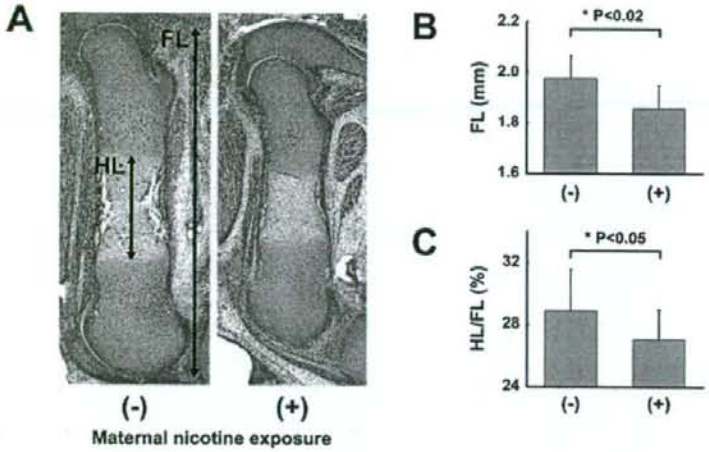


**Figure 5. Maternal nicotine exposure in wild-type mice.** Ovulation-induced pregnant mice were mated and were given drinking water with nicotine during pregnancy. At noon on gestational day 15, the fetuses were sacrificed, and their legs were histologically investigated. A: Skeletal growth estimated by measuring the femur length (FL) and the length of the hypertrophic zone of the femur (HL). B: FL (mm), C: HL/FL (%) of E15.5 fetuses whose mothers were given drinking water with or without nicotine. Nicotine significantly decreased FL and HL/FL.
doi:10.1371/journal.pone.0003945.g005

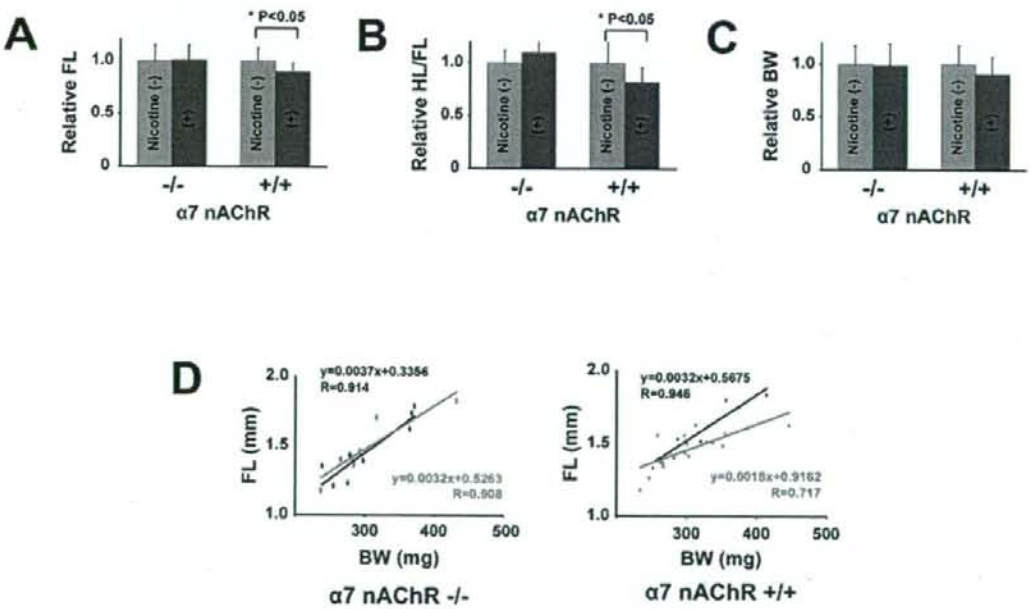


**Figure 6. Maternal nicotine exposure in alpha7 nAChR-disrupted mice.** A–C: FL, HL/FL, and body weight (BW) of alpha7 nAChR −/− and alpha7 nAChR +/+ E15.5 littermate fetuses. Alpha7 nAChR +/− female were mated with alpha7 nAChR +/− male, and given drinking water with or without nicotine during pregnancy. Relative FL, HL/FL, and BW were calculated, each value in mice that did not receive nicotine was regarded as equal to 1.0. Nicotine significantly reduced FL and HL/FL in alpha7 nAChR +/+ fetuses but not in alpha7 nAChR −/− fetuses (A,B). Nicotine did not significantly reduce BW in either genotype (C). D: Scatterplot and correlation between the FL and BW of mice with (red line) or without (black line) exposure to nicotine. In alpha7 nAChR +/+ fetus, Nicotine downwardly shifts the linear slope in alpha7 nAChR +/+ fetuses but not in alpha7 nAChR −/− fetuses.
doi:10.1371/journal.pone.0003945.g006

collagen synthesis of human articular chondrocytes in vitro [21]. Cultured human growth plate chondrocytes derived from infant fingers serve as a good model for analyzing whether nicotine has direct action on growth plate chondrocytes. The present findings of nicotinic effect, i.e. decreasing matrix synthesis and suppressing hypertrophic differentiation but not proliferation on growth plate chondrocytes in vitro, indicate the direct effect of nicotine on growth plate chondrocytes. The findings are consistent with reports that maternal nicotine exposure has a negative effect on endochondral ossification in animals [13]. Besides, these findings are consistent, considering the fact that longitudinal skeletal growth is partly caused by matrix synthesis and hypertrophic differentiation of chondrocytes. Confirmation of the animal model using "human" chondrocytes is essential since certain chemicals, such as thalidomide, exhibit different effects in humans and rodents.

Differences of expression levels of the genes for Col X, ALP, Ihh, MMP13, and VEGF in alginate beads culture (Figure 3B, C) may attribute to differential regulation among hypertrophic markers. Expression of the Ihh, Col X, and ALP genes were down-regulated by nicotine and the MMP13 and VEGF genes remained unaffected. Alternatively, the difference could be a result of chondrocyte culture, that is, artifactual induction ex vivo, and the MMP13 and VEGF genes were indeed expressed at the start of alginate bead culture with chondrocytes at passage 1 (Fig. 3B, lane 1: "0 W"). In contrast, the Col X, ALP, and Ihh genes were appropriately regulated after three-dimensional culture (Figure 3B, lane 2: "3 W"; Figure 3C, lane 1: without exposure to nicotine), as is the case with gene regulation in the growth plate.

### Involvement of alpha7 nAChR in delayed endochondral ossification

The alpha7 nAChR-null mice exhibit normal development, including neural tissue, but alpha7 nAChR-null mice lack nicotinic currents in hippocampal neurons [22], and show abnormalities in late-stage keratinocyte development in the epidermis [23]. Lack of phenotypic abnormality in the femur of fetuses (Figure 5B) and adults indicates that ACh signaling through alpha7 nAChR has little involvement in the process of physiological skeletal growth. Results using MLA, the antagonist to alpha7 nAChR, strongly suggest the involvement of alpha7 nAChR in the nicotinic effect on chondrocytes. Such low-molecular weight substances may, however, have additional unclarified action in addition to any "specific" action. The proof of alpha7 nAChR involvement in delayed skeletal growth was strengthened by the in vivo experiments with alpha7 nAChR gene-disrupted mice. Especially so, considering the fact that maternal nicotine exposure caused delayed skeletal growth in only alpha7 nAChR +/+ fetuses compared with their alpha7 nAChR −/− littermates, fetal alpha7 nAChR but not maternal alpha7 nAChR is responsible for the mechanism of nicotine-induced delayed skeletal growth.

Since nicotine exposure has been reported to be epidemiologically and experimentally correlated with maternal effect, i.e., abnormal placental function and blood flow [10], the physiological and pathological function of alpha7 nAChR in growth plate was confirmed by comparing "littermates" of alpha7 nAChR (Figure 6B). This comparison confirms involvement of alpha7 nAChR on the fetus, and eliminates a possibility of maternal effect. Furthermore, decrease of relative femur length (Figure 6C, scatterplot and correlation, right panel, alpha7 nAChR +/+) and lack of nicotinic effect on body weight of alpha7 nAChR fetuses (Figure 6B, right panel, "BW") by maternal nicotine exposure indicate a specific effect of nicotine on bone growth rather than a systemic effect. Therefore, the effect of smoking during pregnancy on skeletal growth may be attributed to this direct action of nicotine on growth plate chondrocytes, at least in part.

Our studies suggest that, from the large number of chemicals associated with cigarette smoking, nicotine may cause delayed skeletal growth and, indeed, amniotic fluid and breast milk both have higher concentrations of nicotine than maternal serum does [24]. In addition, metabolism of nicotine in the fetus and child is much slower than that in adults [25]. We therefore should pay close attention to the effect of smoking, regardless of being active or passive, on growth plate chondrocytes. This nicotinic effect may also extend to the delay of fracture repair or generation of non-union in adults, since the process of bone repair also partly depends on endochondral ossification.

## Materials and Methods

### Chondrocyte cultures

Human chondrocytes were isolated from epiphysis of extra fingers, which were surgically excised from patients with polydactyly. Ethical approval for tissue collection was granted by the Institutional Review Board of the National Research Institute for Child Health and Development, Tokyo, Japan (#88). Minced tissue was incubated for 1 h at 37°C in 0.08% trypsin in PBS, then for 6 h at 37°C in 0.2% collagenase type 1 (Wako, Osaka, Japan) in Dulbecco's Modified Eagle's medium (DMEM). The released cells were washed and resuspended in DMEM containing 10% fetal bovine serum (FBS, Sanko Junyaku Co., Tokyo, Japan, lot number: 27110307) and plated at a density of $1\times10^6$ cells per 100 mm dish for primary monolayer cultures, or $1\times10^6$ cells per 35 mm dish for calcium influx assay and immunocytochemical assay of nAChR. In each experiment, we used one lot of cultured chondrocytes from extra fingers obtained from four patients.

### RT-PCR for detection of nAChR subunit

Total RNA was prepared from epiphysis of extra fingers using Isogen (Nippon Gene) according to the manufacturer's recommendations. DNase-treated RNA was reverse transcribed in 20 µl of RT-PCR mix (50 mM Tris, pH 8.3, 3 mM $MgCl_2$, 75 mM KCl, 50 mM dNTPs, 2.5 µM oligo$(dT)_{20}$, 5 mM DTT, 2 U RNaseOUT and 10 U SuperScriptIII (Invitrogen) at 50°C for 1 h. The PCR was performed in a final volume of 50 µl containing 1 µl of the single strand cDNA product, 25 mM TAPS (pH 9.3), 50 mM KCl, 2.0 mM $MgCl_2$, 1 mM β-mercaptoethanol , 200 µM dNTPs, and AmpliTaq Gold (Applied Biosystems) and 20 pmol of each forward (5′) and reverse (3′) primers (Table S1). For each experiment the housekeeping gene GAPDH was amplified with 25–35 cycles to normalize the cDNA content of the samples. The amplification was performed for 30 cycles, with other conditions following polymerase-producing manufacturer's recommendations. Human brain and skeletal muscle RNAs were purchased from Ambion (Austin, TX).

### Western blot analysis for detection of nAChR subunit

Total proteins were isolated from primary monolayer cultures using CelLyticTM-M Mammalian Cell Lysis/Extraction Reagent (Sigma). The proteins were separated by SDS-PAGE (Bio-Rad) in a 10% acrylamide gel, then blotted at 60 V for 2 h at 4°C onto a nitrocellulose membrane. Non-specific binding was blocked by incubation in TBS containing 10% BSA and 0.05% Tween-20. The membrane was subsequently incubated at 4°C overnight with the monoclonal antibody to nicotinic acetylcholine receptor, alpha7 subunit (Sigma, St-Louis, MO; product number: N 8158) diluted 1:3000. After rinsing, the membrane was incubated for 1 h at room temperature in horseradish peroxidase-conjugated rabbit

anti-rat IgG antibody (Sigma; A 5795) at a dilution of 1:3000 in TBS containing 0.05% Tween-20. After rinsing, the membrane was immersed in ECL solution (GE Healthcare, Buckinghamshire, UK). Then, the blots were visualized by LAS-1000plus IDX2, the luminescent image analyzer (Fuji Photo Film, Japan).

### Immunocytochemical and immunohistochemical analysis

Immunocytochemical analysis was performed as previously described [26]. Briefly, dishes were incubated with antibody to alpha7 subunit of nAChR in PBS containing 1% BSA. As a methodological control, the primary antibody was omitted. After washing in PBS, dishes were incubated with horseradish peroxidase (HRP)-conjugated rabbit anti-rat IgG antibody. Staining was developed by using a solution containing diaminobenzidine and 0.01% $H_2O_2$ in 0.05 M Tris-HCl buffer, pH 6.7.

For immunohistochemical analysis, hind legs of E15.5 C57BL/6J mice were prepared, fixed in 4% paraformaldehyde phosphate buffer solution (Wako) overnight at 4°C, and embedded in paraffin. Immunohistochemical analysis was performed as previously described [27]. Briefly, slides were treated with 0.4% pepsin (DAKO) at 37°C for 30 min, incubated with primary antibody to alpha7 subunit of nAChR(Sigma, product number: N 8158) diluted 1:2000 in PBS containing 1% BSA at room temperature for 3 h, and incubated with simple mouse stain MAX-PO (RAT), a second antibody, at room temperature for 1 h. Staining was developed by using a solution containing diaminobenzidine and 0.01% $H_2O_2$ in 0.05 M Tris-HCl buffer, pH 6.7. Finally, slides were counterstained with hematoxylin.

### Agarose gel cultures

Chondrocytes were cultured in agarose-stabilized suspension using a modified method as previously described [28]. Primary monolayer cultures were trypsinized, re-suspended in agarose gel medium : DMEM/F-12 containing 10% FBS, 100 units/ml penicillin G, 100 mg/ml streptomycin, and 50 mg/ml ascorbate, to a concentration of $2\times10^4$ cells/ml, then mixed with equal volume of 1% low-temperature melting agarose (Sigma-Aldrich, Steinheim, Germany) in agarose gel medium, giving a final concentration of $1\times10^4$ cells/ml suspended in 0.5% low-temperature melting agarose in agarose gel medium (suspension agarose). Three milliliters of suspension agarose were added to 60 mm culture plates that were precoated with 2 ml of 1% autoclaved standard agarose (Bio-Rad, Hercules, CA). The gel was allowed to solidify at 4°C before addition of agarose gel medium. Then, culture plates were placed in a 37°C, 5% $CO_2$ humidified incubator for 21 days, and medium containing indicated concentration of nicotine was replaced once at the beginning of the week. After 21 days, suspension agarose was transferred to a glass slide, and placed on a plate warmer at 50°C with a covering of positively-charged nylon membranes (Roche, Mannheim, Germany). The slides were completely dried in a incubator at 42°C overnight, and fixed in 4% paraformaldehyde for 15 min, and stained with ALB to identify colonies producing glycosaminoglycans and to observe histologically. Colonies were defined as a cluster of cells with a diameter greater than 50 μm. ALP activity was determined in non-fixed agarose slide by Histofine, ALP substrate kit (Nichirei, Tokyo, Japan) following the manufacturer's product information. Type 10 collagen expression was also determined in the agarose slide using specific monoclonal antibody (Sigma; product number: C7974). The slide was fixed in acetone (Nacalai Tesque, Kyoto, Japan) at room temperature for 20 min. Non-specific binding was blocked with 2.5% normal rabbit serum (DakoCytomation, Glostrup, Denmark) in PBS containing 1% BSA and 1% Triton X-100. Slides were incubated for 6 h at room temperature with primary antibody, diluted 1:2000 in PBS containing 1% BSA. Bound antibody was detected by HRP-conjugated polyclonal rabbit anti-mouse IgM antibody (Dako, Glostrup, Denmark; product number: P 0260) diluted 1:100 in PBS at room temperature for 30 min. Peroxidase activity was visualized with diaminobenzidine tetrahidrochloride plus 0.03% $H_2O_2$, and slide was counterstained with hematoxylin.

### Alginate bead cultures

Chondrocytes were cultured in alginate beads following the method described by De Ceuninck et al. Primary monolayer cultures were trypsinized, washed, and centrifuged. The isolated chondrocytes were suspended at a concentration of $2\times10^6$ cells/ml in a 1.25% alginate in 0.15 M NaCl. The cell suspension was slowly expressed through a 21 gauge needle and dropped into a 102 mM $CaCl_2$ solution. The beads with approximately 25,000 cells/bead were allowed to polymerize for 10 min and washed three times with 0.15 M NaCl, followed by two washes in DMEM/F12. The beads were then transferred to medium (200 beads/10 ml/60 mm culture dish): DMEM/F-12 containing 10% FBS, 50 μg/ml ascorbate, 100 units/ml penicillin G, 100 mg/ml streptomycin. The beads were cultured at 37°C in a 5% $CO_2$ humidified incubator for four months, and medium with or without nicotine was replaced twice weekly. The beads were transferred to new dishes every other week to avoid the formation of monolayer cultures on the bottom of the dish by chondrocytes escaping from the beads.

For histological analysis, the beads were fixed in 4% paraformaldehyde, 0.1 M cacodylate buffer, pH 7.4, containing 10 mM $CaCl_2$ for 4 h at room temperature, and then washed overnight at 4°C in 0.1 M cacodylate buffer, pH 7.4, containing 50 mM $BaCl_2$. The beads were dehydrated through alcohols and embedded in paraffin. The sections were routinely stained with ALB and safranin-O.

For RT-PCR analysis, chondrocytes were separated from the beads by incubating the beads in dissolution solution (at a ratio of 200 μl/bead), containing 55 mM EDTA, for 5 min and centrifuged. Total RNA was isolated by using RNeasy (Qiagen) following manufacturer's instructions, and was converted to cDNA by same method as described above. The sequences of PCR primers of human chondrocyte-related gene are listed in Table S2. PCR was performed in a final volume of 50 μl containing 2 μl of the single strand cDNA product (10 ng/μl), 10 mM Tris-HCl (pH8.3), 50 mM KCl, 1.5 mM $MgCl_2$, 200 μM dNTPs, 1.25 U Taq (Takara), and 20 pmol of each forward (5′) and reverse (3′) primers.

### Calcium imaging

Primary monolayer cultures in 35 mm glass-bottomed plates were prepared. At near confluence, measurement was done by using Fluo-4 NW calcium assay kit (Molecular Probes, product number: F36206) following the manufacturer's product information. In short, the cells were incubated in dye loading solution containing 2.5 mM probenecid at 37°C for 30 min, then at room temperature for an additional 30 min before nicotine stimulation. The fluorescence was measured in LSM 510 (Carl Zeiss) with the settings appropriate for argon laser. Nicotine and its antagonists were prepared as a solution in assay buffer. If antagonists were used, they were added 30 min prior to nicotine stimulation.

### Maternal nicotine exposure in wild-type mice

Three-month-old pregnant mice were purchased at day 1 of pregnancy from Sankyo Laboratories (Tokyo, Japan). The mice were given drinking water containing 2% sucrose (Wako, Osaka, Japan) with or without nicotine (hydrogen tartrate salt; Sigma-